

RESEARCH ARTICLE

The genetic basis of natural variation in the timing of vegetative phase change in *Arabidopsis thaliana*

Erin Doody, Yuqi Zha, Jia He and R. Scott Poethig*

ABSTRACT

The juvenile-to-adult transition in plants is known as vegetative phase change and is marked by changes in the expression of leaf traits in response to a decrease in the level of miR156 and miR157. To determine whether this is the only mechanism of vegetative phase change, we measured the appearance of phase-specific leaf traits in 70 natural accessions of *Arabidopsis thaliana*. We found that leaf shape was poorly correlated with abaxial trichome production (two adult traits), that variation in these traits was not necessarily correlated with the level of miR156, and that there was little to no correlation between the appearance of adult-specific vegetative traits and flowering time. We identified eight quantitative trait loci controlling phase-specific vegetative traits from a cross between the Columbia (Col-0) and Shaktara (Sha) accessions. Only one of these quantitative trait loci includes genes known to regulate vegetative phase change (*MIR156A* and *TOE1*), which were expressed at levels consistent with the precocious phenotype of Sha. Our results suggest that vegetative phase change is regulated both by the miR156/SPL module and by genes specific to different vegetative traits, and that natural variation in vegetative phase change can arise from either source.

KEY WORDS: miR156/SPLs, Vegetative phase change, Natural variation, Quantitative trait mapping

INTRODUCTION

In land plants, shoot growth can be divided into several distinct developmental phases. Following germination, a plant begins a period of juvenile vegetative growth, a developmental phase that can be very short or last years (Wareing, 1959). It then transitions to an adult vegetative growth pattern, in a process known as vegetative phase change. The vegetative-to-reproductive transition usually occurs after vegetative phase change (although it can occur during the juvenile phase), and is accompanied by the production of structures involved in sexual reproduction, such as flowers or cones (Levy and Dean, 1998; Amasino, 2010; Huijser and Schmid, 2011; Andrés and Coupland, 2012). Finally, to complete its life cycle, a plant undergoes senescence and dies (Leopold, 1961; Thomas et al., 2003). The duration of these phases is highly variable between and within plant species, and transitions between them are dependent on both endogenous developmental pathways and environmental cues (Conway and Poethig, 1993; Scheres and van der Putten, 2017).


The traits associated with vegetative phase change vary between species, but include changes in leaf shape and shoot architecture, photosynthesis, immune and defense responses, stress responses and other processes (Allsopp, 1967; Hackett, 1985; Poethig, 1990; James and Bell, 2001; Boege and Marquis, 2005; Stief et al., 2014; Cui et al., 2014; Nguyen et al., 2017; Leichter and Poethig, 2019; Lawrence et al., 2021). In *Arabidopsis thaliana*, the most obvious morphological markers of vegetative phase are a decrease in leaf base angle, the production of trichomes on the abaxial surface of the leaf blade, and an increase in the number and size of serrations of the leaf margin (Telfer et al., 1997).

The master regulators of vegetative phase change are the closely related microRNAs miR156 and miR157 (Wu et al., 2009). miR156 and miR157 are highly expressed in leaves produced early in development and at much lower levels in leaves produced during the adult phase (He et al., 2018a). This decrease allows for an increase in their targets, the SQUAMOSA PROMOTER BINDING-LIKE (SPL) transcription factors, which in turn regulate many different processes associated with shoot and leaf development (Wang and Wang, 2015; Xu et al., 2016). One of the transcriptional targets of SPL proteins is *MIR172B* (Wu et al., 2009), which represses several members of the AP2/TOE family of transcription factors (Aukerman and Sakai, 2003; Chen, 2004). Although miR172, AP2 and TOE are best known as regulators of flowering time (Aukerman and Sakai, 2003; Zhu and Helliwell, 2011), they also control the production of some adult leaf traits, such as abaxial trichomes (Wang et al., 2019; Xu et al., 2019). Regulation of vegetative development by the miR156/SPL module is conserved across land plants of varying complexity and evolutionary age (including mosses and liverworts), short-lived annuals such as *A. thaliana*, and long-lived perennials such as trees (Mishler, 1986; Axtell and Bowman, 2008; Wang et al., 2011; Tsuzuki et al., 2019; Zhang et al., 2020; Aloni, 2021).

Although many aspects of the regulation of vegetative phase change by the miR156/7 pathway have been uncovered through a molecular genetic approach, many questions remain unanswered. In particular, the genetic basis for natural intra- and interspecies variation in the timing of vegetative phase change, or its relationship to the reproductive phase transition remains to be determined (Foerster et al., 2015; Goebel, 1900; Hudson et al., 2014; Wiltshire et al., 1991). Studies of natural variation in *A. thaliana* have been vital for understanding the mechanism of flowering time (Alonso-Blanco et al., 1998; Lempe et al., 2005; Shindo et al., 2005; Rosas et al., 2014), germination (Chiang et al., 2009; Martínez-Berdeja et al., 2020), senescence (Churchill and Doerge, 1994; He et al., 2018b) and many other phenomena (Bergelson and Roux, 2010; Rubin et al., 2019; Sasaki et al., 2019; Yuan and Kessler, 2019; González et al., 2020; Nakano et al., 2020). For example, these studies have revealed that natural variation in flowering time is attributable primarily to two genes, *FRI* and *FLC* (Alonso-Blanco et al., 1998; Gazzani et al., 2003; Lempe et al., 2005). *FLC* has also

Biology Department, University of Pennsylvania, Philadelphia, PA 19104, USA.

*Author for correspondence (spoethig@sas.upenn.edu)

 E.D., 0000-0002-1282-1792; R.S.P., 0000-0001-6592-5862

Handling Editor: Ykä Helariutta

Received 4 November 2021; Accepted 19 April 2022

been found to have a slight effect on vegetative development (Willmann and Poethig, 2011). However, the extent to which the timing of vegetative phase change varies within *A. thaliana* – or any other species – as well as the genetic basis for natural variation in this process, are largely unknown.

To begin to unravel these questions, we grew a group of 70 genome-sequenced natural accessions of *A. thaliana* in uniform conditions and characterized variation in vegetative phase change. This analysis revealed that expression of different phase-specific vegetative traits is not tightly correlated in these accessions and is unrelated to variation in flowering time in non-photoinductive (short day; SD) and photoinductive (long day; LD) conditions. We then performed a more detailed analysis of a group of Central Asian accessions with precocious leaf shape development collected from environments characterized by high variation in temperature. We found that about half of these precocious accessions had relatively low levels of miR156, whereas the other half had approximately the same, or more miR156 than our standard accession, Columbia (Col-0). Quantitative trait locus (QTL) mapping of phase-specific vegetative traits using recombinant inbred lines derived from a cross between Col-0 and one of these accessions, Shakdara (Sha), produced eight QTLs. One of these QTLs contains two loci – *MIR156A* and *TOE1* – known to regulate vegetative phase. Both of these genes are expressed at significantly lower levels in Sha than in Col-0, which is consistent with the difference in the timing of vegetative phase change in these accessions. The other seven QTLs did not contain genes known to regulate vegetative phase change.

Together, our results indicate that natural variation in the timing of vegetative phase change is regulated both by variation in miR156 and by genes that operate independently of miR156 to control the expression of specific vegetative traits.

RESULTS

Natural accessions of *A. thaliana* show variation in the timing of vegetative phase change

To survey the phenotypic diversity in the timing of vegetative phase change in natural accessions, we selected a group of 70 accessions to represent the geographic and ecological diversity of this species (Fig. 1A) and grew them under SD and LD conditions. Plants were scored for the timing of vegetative phase change by measuring the angle of the base of the lamina (leaf base angle) and by counting the number of leaves lacking abaxial trichomes. Because abaxial trichome production is a qualitative trait, the node at which the shoot switches from the juvenile (absent) to the adult (present) form of this trait is easy to determine. In contrast, the angle of the leaf base becomes gradually smaller from leaf to leaf, making it difficult to specify a single node at which the juvenile-to-adult transition occurs (Fig. S1A). We measured the angle of the leaf base of leaf 4 on the assumption that accessions with a small leaf base angle at this node undergo vegetative phase change earlier than accessions with a larger leaf base angle.

We found that accessions varied widely in their leaf 4 base angle (Fig. 1B) and that the appearance of abaxial trichomes varied from leaf 3 to leaf 18 in SD conditions (Fig. 1C). Although the

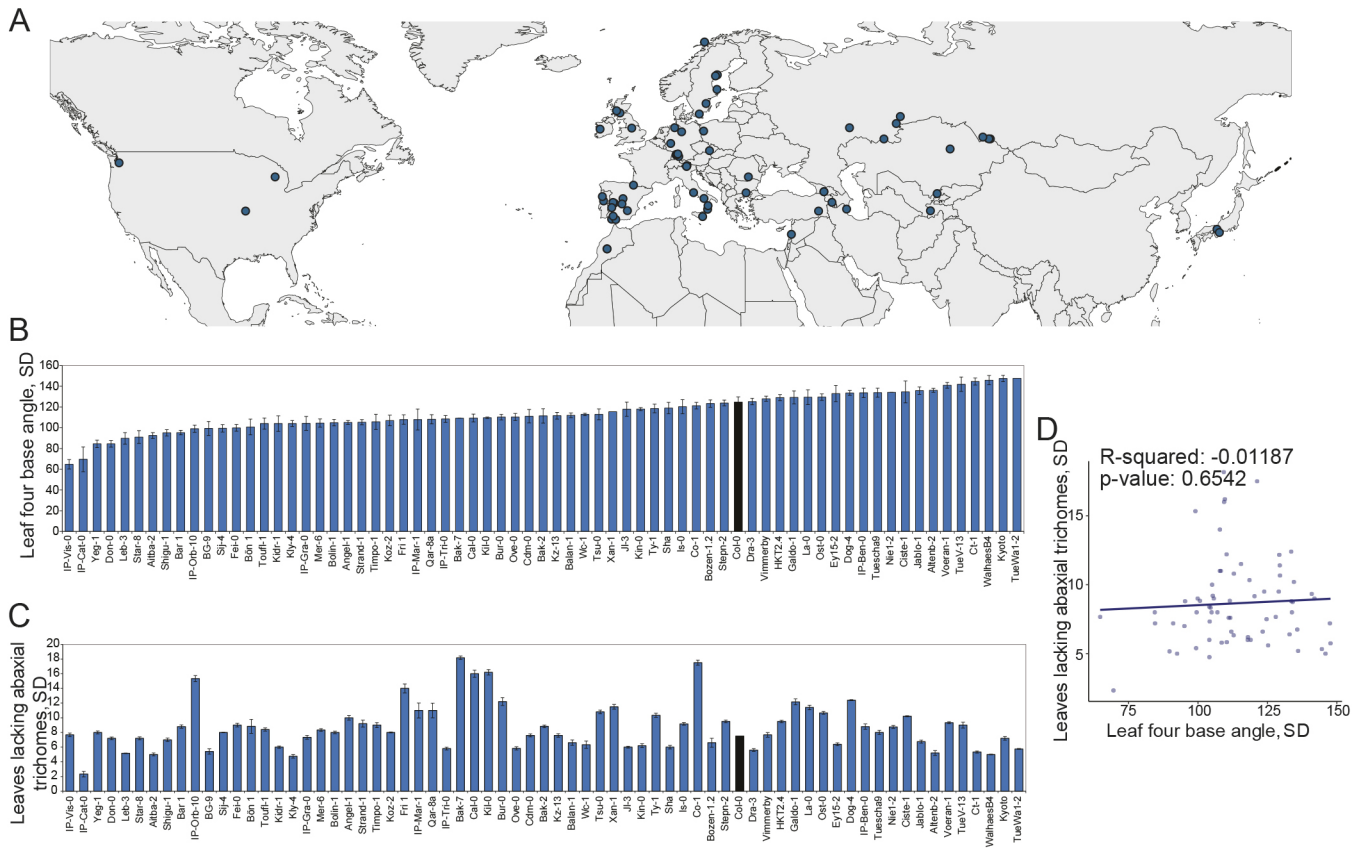


Fig. 1. Phenotypic analysis of *A. thaliana* natural accessions in SD. (A) Collection locations of the 70 natural accessions used in this study. (B) Leaf 4 base angle of natural accessions grown in SD conditions. (C) Number of juvenile leaves, indicated by leaves lacking abaxial trichomes, in natural accessions grown in SD conditions, in the same order as B. In B,C, Col-0 is shown in black. (D) Correlation of leaf 4 base angle with leaves lacking abaxial trichomes in natural accessions grown in SD conditions. Linear regression is represented by a solid blue line; R^2 and P -value are indicated above.

base angle of leaf 4 was strongly correlated in SD and LD (Fig. S1B), there was no correlation between the angle of the leaf base and the first leaf with abaxial trichomes (Fig. 1D). This suggests that traits associated with the timing of vegetative phase change are regulated by at least partially different mechanisms in these accessions.

To examine the relationship between these leaf developmental traits and the reproductive transition, we grew the same accessions in LD conditions. Because these accessions have differing rates of leaf initiation, total leaf number is not necessarily an accurate measure of flowering time (Fig. S2A). Consequently, we used days to first open flower as a measure of flowering time. This trait is highly correlated with days to bolting (Fig. S2B-D), but is less correlated with rosette leaf number (Fig. S2E,F).

Similar to what we found in SD, leaf 4 base angle and the number of leaves lacking abaxial trichomes varied considerably in LD (Fig. 2A,C) and there was no correlation between these two traits. There was also no relationship between leaf 4 base angle and days to first open flower in either SD or LD (Fig. 2A,B, Fig. S1D). We did observe moderate correlation between production of abaxial trichomes and days to flower in LD (Fig. 2D), but not in SD (Fig. 2F), even though the appearance of abaxial trichomes is highly correlated between SD and LD (Fig. S1C). This may be attributable to the effect of floral induction on the expression of AP2-like transcription factors, which regulate both flowering

time and abaxial trichome production (Wang et al., 2019; Xu et al., 2019). Importantly, these results indicate that photoperiod can affect the temporal relationship between different phase-specific traits.

Accessions from Central Asia produce adult leaves precociously

Within this group of accessions, we focused on a group of nine accessions from Central Asia that had a similar early adult leaf-shape phenotype (Fig. 3A,D,E). Principal component analysis (PCA) performed on 19 bioclimatic variables plus altitude from the WorldClim database (<https://www.worldclim.org/>) revealed that these Central Asian accessions were collected from regions with similar climates. These regions were positively correlated with temperature seasonality and temperature range, two measurements of high variation in temperature (Fig. 3B,C), suggesting that these environmental factors promote the development of adult leaf shape. However, as we saw in the larger group of accessions, appearance of early adult leaf shape and production of abaxial trichomes were de-coupled. Only four of these accessions produced abaxial trichomes significantly earlier than Col-0, whereas the others produced abaxial trichomes at the same time or slightly later than Col-0 (Fig. 3E,F). This provides further evidence that different phase-specific traits are regulated by different mechanisms in *A. thaliana*.

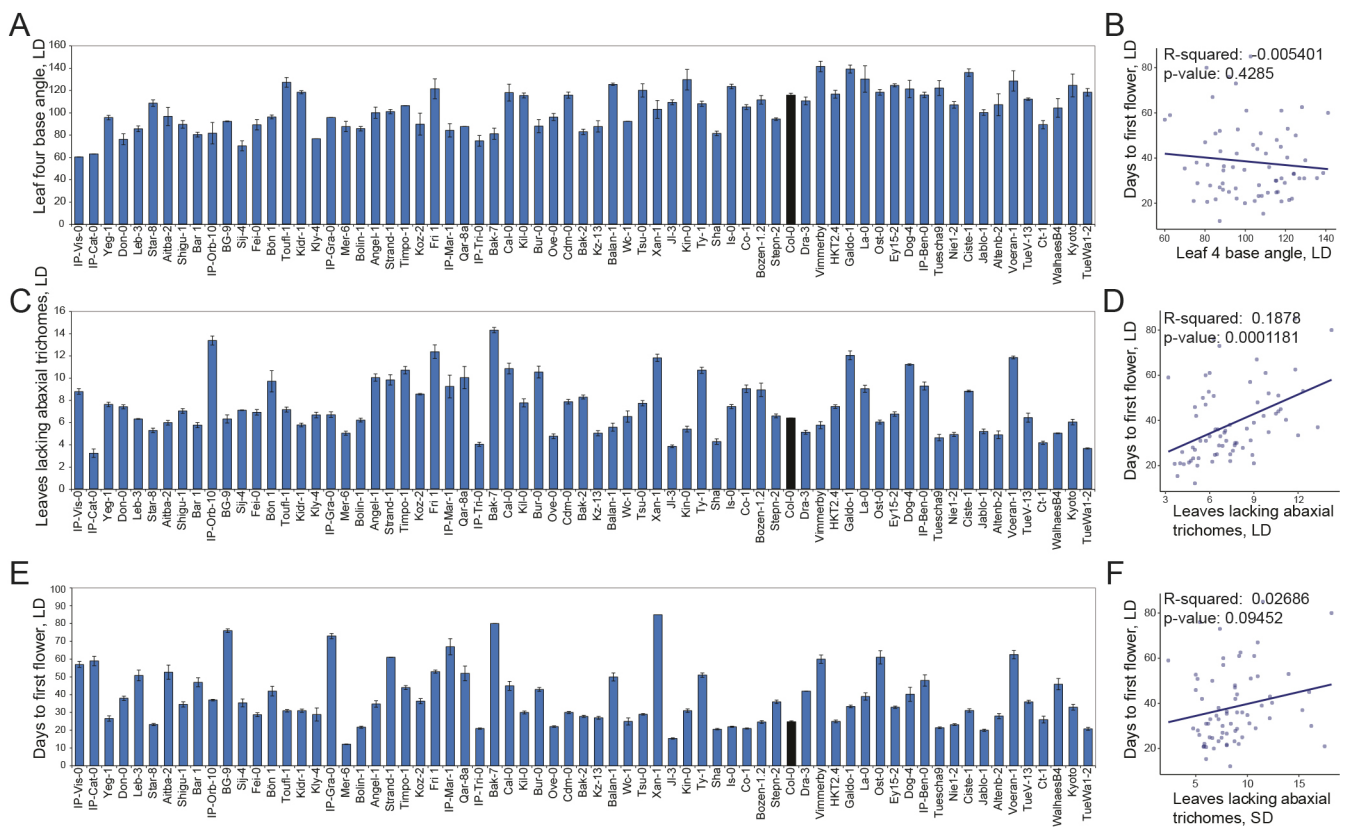


Fig. 2. Phenotypic analysis of *A. thaliana* natural accessions in LD. (A) Leaf 4 base angle of natural accessions grown in LD conditions, in the same order as Fig. 1B. (B) Correlation of leaf 4 base angle with days to first flower in natural accessions grown in LD conditions. Linear regression is represented by solid line; R^2 and P -value are indicated above. (C) Number of juvenile leaves, indicated by leaves lacking abaxial trichomes, in natural accessions grown in LD conditions, in the same order as Fig. 1B. (D) Correlation of number of leaves lacking abaxial trichomes with days to first flower in natural accessions grown in LD conditions. Linear regression is represented by solid line; R^2 and P -value are indicated above. (E) Days to first flower of natural accessions grown in LD, in the same order as Fig. 1B. (F) Correlation between the number of leaves lacking abaxial trichomes in SD with days to first flower grown in LD in natural accessions. Linear regression is represented by solid line; R^2 and P -value are indicated above. In A,C,E, Col-0 is shown in black.

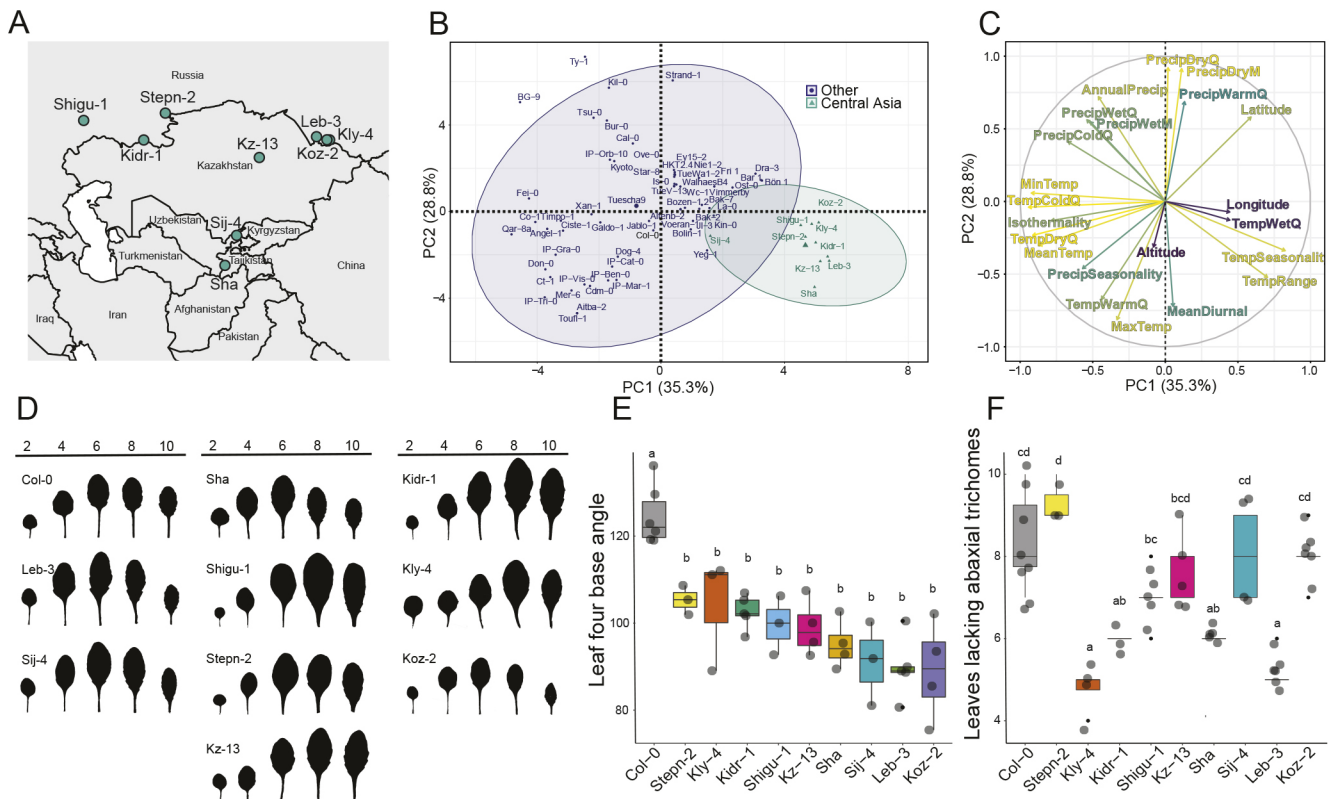


Fig. 3. Phenotypic analysis of natural accessions from Central Asia that undergo early vegetative phase change. (A) Collection locations of natural accessions from Central Asia with early adult leaf shape. (B,C) PCA score plot (B) and loading plot (C) for 19 bioclimatic variables and altitude for collection locations of 70 *A. thaliana* accessions. Percentages of variance indicated on each PCA axis. Accessions are colored to show Central Asian accessions. (D) Fully expanded rosette leaves 2, 4, 6, 8 and 10 of natural accessions from Central Asia under SD conditions. (E,F) Leaf 4 base angle (E) and the number of leaves lacking abaxial trichomes (F) of early Central Asian natural accessions ($n \geq 3$ for each genotype). Significantly distinct groups (denoted by letters) were determined by one-way ANOVA followed by Tukey HSD test ($P=0.05$). Gray circles indicate biological replicates; black dots indicate outliers; center line marks the median value; boxes outline the first and third quartiles; whiskers mark minimum and maximum values.

Variation in miR156/SPL gene expression does not fully explain natural phenotypic variation in vegetative phase change in Central Asian accessions

To investigate the role of miR156 in these accessions, we measured the abundance of the mature miR156 transcript and the primary transcripts of *MIR156A* and *MIR156C*, which account for about 80% of miR156 pool in Col-0, in the primordia of leaves 1&2. We found that the level of the mature miR156 was lower than Col-0 in about half of the Central Asian accessions that showed early leaf shape development: Leb-3, Stepn-2, Sha and Kly-4. However, the other five accessions had Col-0-like abundance of miR156, which is the opposite of the expected result, as high levels of miR156 promote juvenile traits (Fig. 4A). Two accessions with both early leaf shape and abaxial trichome development – Shigu-1 and Kidr-1 – did not have decreased levels of mature miR156 relative to Col-0. Furthermore, the expression of pri-miR156A and pri-miR156C was not fully correlated with the timing of the vegetative phase transition, or with the level of the mature miR156 transcript in all of these accessions (Fig. 4B,C). For example, Koz-2 and Shigu-1 both had approximately the same amount of miR156 in leaves 1&2 as Col-0, but both pri-miR156A and pri-miR156C were significantly lower in these accessions than in Col-0. However, three accessions (Sha, Kly-4 and Leb-3) all had lower levels of mature miR156 and the primary transcripts of *MIR156A* and *MIR156C* compared with Col-0, which suggests that miR156 may have a role in regulating vegetative phase change in these accessions (Fig. 4).

To determine whether the precocious phase change phenotype of these accessions is regulated downstream of miR156, we measured the abundance of six miR156 targets – *SPL3*, *SPL5*, *SPL9*, *SPL10*, *SPL11* and *SPL15* – in the primordia of leaves 1&2. These six genes include all of the SPLs that have an effect on the timing of vegetative phase change, except for *SPL13* and *SPL2* (Xu et al., 2016). Although *SPL13* is an important regulator of vegetative phase change in Col-0, this ecotype possesses a recent tandem duplication of this locus that is absent in many natural accessions (Xu et al., 2016). This results in a roughly twofold difference in *SPL13* expression between Col-0 and these accessions, and makes it an unreliable measure of vegetative phase change when comparing to Col-0 (Xu et al., 2016). We did not measure the expression of *SPL2* because it is highly polymorphic in these accessions, suggesting that it is not likely to be an important regulator of vegetative phase change.

There was no clear relationship between the abundance of these transcripts and the expression of miR156 or their phase change phenotype (Fig. 5). Seven of the nine lines had significantly less *SPL15* than Col-0 and eight had approximately the same amount of *SPL9* as Col-0, even though many of these accessions had lower levels of miR156 than Col-0. Shigu-2 had elevated levels of *SPL3*, *SPL5*, *SPL9*, *SPL10* and *SPL11* compared with Col-0, which correlates with its early phase change phenotype, but not with the amount of miR156 in this accession. A few other accessions had one elevated SPL gene (Kly-4 and *SPL3*; Kidr-1 and *SPL5*; Sha and

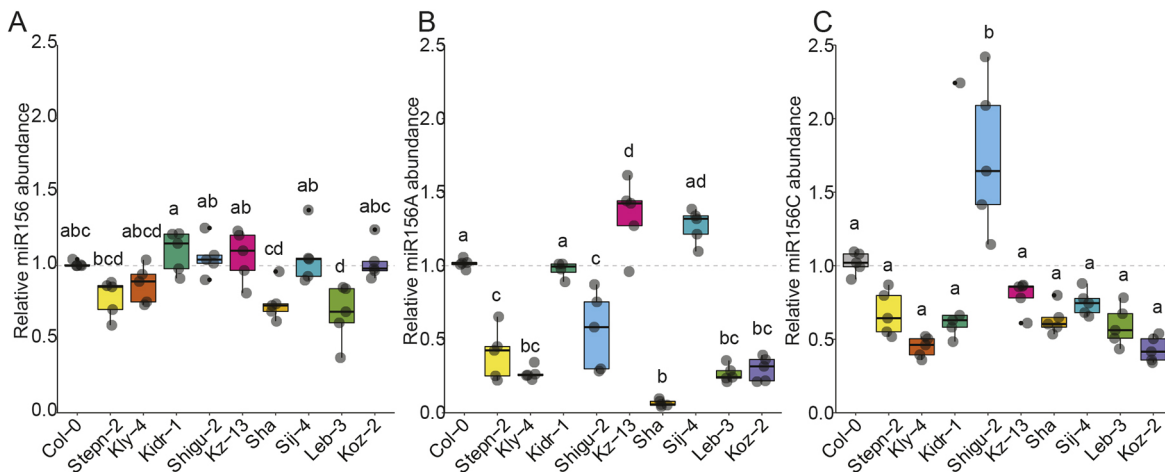


Fig. 4. Relative abundance of mature miR156 and miR156 primary transcripts in leaf primordia of early Central Asian accessions. (A) Mature miR156 abundance relative to SnoR101 in the primordia of leaves 1&2 in Central Asian accessions in same order as Fig. 3E. (B,C) The abundance of the pri-*miR156A* and pri-*miR156C* primary transcripts in the primordia of leaves 1&2 of Central Asian accessions. Accessions are in the same order as in Fig. 3E ($n=5$). Significantly distinct groups (denoted by letters) were determined by one-way ANOVA followed by Tukey HSD test ($P=0.05$). Gray circles indicate biological replicates; black dots indicate outliers; center line marks the median value; boxes outline the first and third quartiles; whiskers mark minimum and maximum values.

SPL15), but there was not an obvious pattern of *SPL* gene expression across this group of accessions.

Together, these data indicate that regulation of phase-specific aspects of leaf shape and the production of abaxial trichomes is complex, even among accessions with similar geographic and climatic origins and vegetative phase change phenotypes. Although some of these accessions, such as Sha, Kly-4 and Leb-3, have the expected decreased levels of miR156 or elevated *SPL* gene expression, the early vegetative phenotype of many of these accessions did not reflect the abundance of miR156 or *SPL* transcripts. This suggests that natural variation in phenotypic traits associated with vegetative phase change is controlled at multiple levels, which could involve a combination variation in the genes that encode miR156 and *SPL* transcription factors, in addition to other unknown genetic loci.

Recombinant inbred lines from Sha×Col-0 reveal eight QTLs that regulate vegetative phase change

Of the accessions from Central Asia, Sha was one of the most consistently precocious in that it had an earlier change in leaf morphology, fewer leaves lacking abaxial trichomes and an earlier increase in leaf serrations compared with Col-0 (Fig. 6A-E). Despite this precocious vegetative phenotype, Sha flowered slightly later than Col-0 after 4 weeks of vernalization (Fig. 6F,G). Additionally, the early vegetative phase change phenotype of Sha persisted in the absence of vernalization, which significantly delayed its flowering (Fig. S3A-C). This demonstrates that vegetative phase change and floral induction are regulated independently in this accession.

To examine the basis for this phenotype, we measured transcript levels of miR156, pri-*miR156A* and pri-*miR156C* in Sha in 2-week-old seedlings, and in the primordia of leaves 1&2 and leaves 5&6 (Fig. 7A). As expected, Col-0 and Sha had relatively high levels of these transcripts in seedlings and leaves 1&2, but had much lower levels in leaves 5&6 (Fig. 7A-C). Sha had significantly less mature miR156, pri-*miR156A* and pri-*miR156C* than Col-0 in seedlings and leaves 1&2, but had essentially the same amount of these transcripts as Col-0 in leaves 5&6, which are produced after Sha has undergone vegetative phase change. This indicates that miR156 either drops more rapidly or is, overall, less abundant in Sha than in Col-0.

Additionally, the observation that leaf 5 has the same level of miR156 in Sha as in Col-0 and yet has a more adult phenotype may indicate that Sha has a lower sensitivity to miR156, i.e. similar levels of miR156 may have a more dramatic impact on *SPL* gene expression and leaf development in Sha than in Col-0. Downstream of miR156, *SPL15* was expressed at a significantly higher level in Sha compared with Col-0 (Fig. 7F). *SPL9* transcripts were consistently, but not significantly, higher in Sha in each of the three samples we examined, but *SPL3* was expressed at similar levels in Sha and Col-0 (Fig. 7D,E). Taken together, these results suggest that the miR156/*SPL* pathway plays a role in the early phase change phenotype of Sha and made it a candidate for further QTL analysis.

To do this, we took advantage of a set of 164 genotyped recombinant inbred lines (RILs) generated from the F2 progeny of a cross between Sha and Col-0 (Fig. 8A-C) (Simon et al., 2008). Ten plants of each line were grown in SD conditions and scored for the leaf 3 base angle, the number of leaves lacking abaxial trichomes, and the number of serrations on leaf 7. Phenotypic data were analyzed using the R/qtl package (Broman et al., 2003).

QTL analysis of the number of leaves lacking abaxial trichomes revealed four significant loci using a confidence interval of 95% (Fig. 8C). The most robustly significant QTL was on the bottom of chromosome 5, and accounted for 20.45% of the variance in the RIL population. A second significant locus on chromosome 2 accounted for 10.84% of the variance. Two less-significant QTLs were found on chromosome 1, accounting for about only ~3% of the variance combined (Fig. 8C). Covariance and QTL interaction analysis revealed the QTL on chromosome 5 was composed of at least two interacting epistatic loci (Fig. 8D,E), but the QTLs on chromosomes 1 and 2 were mostly independent of the others (Fig. S4A-C).

QTL analysis of other traits associated with vegetative phase change produced different results from those found with the number of leaves lacking abaxial trichomes. The most significant peak for leaf 3 base angle was on chromosome 2, and resembled the QTL associated with leaves lacking abaxial trichomes. A second QTL for this trait was located at the top of chromosome 1 (Fig. 9A,B). An analysis of the number of serrations on leaf 7 revealed a single

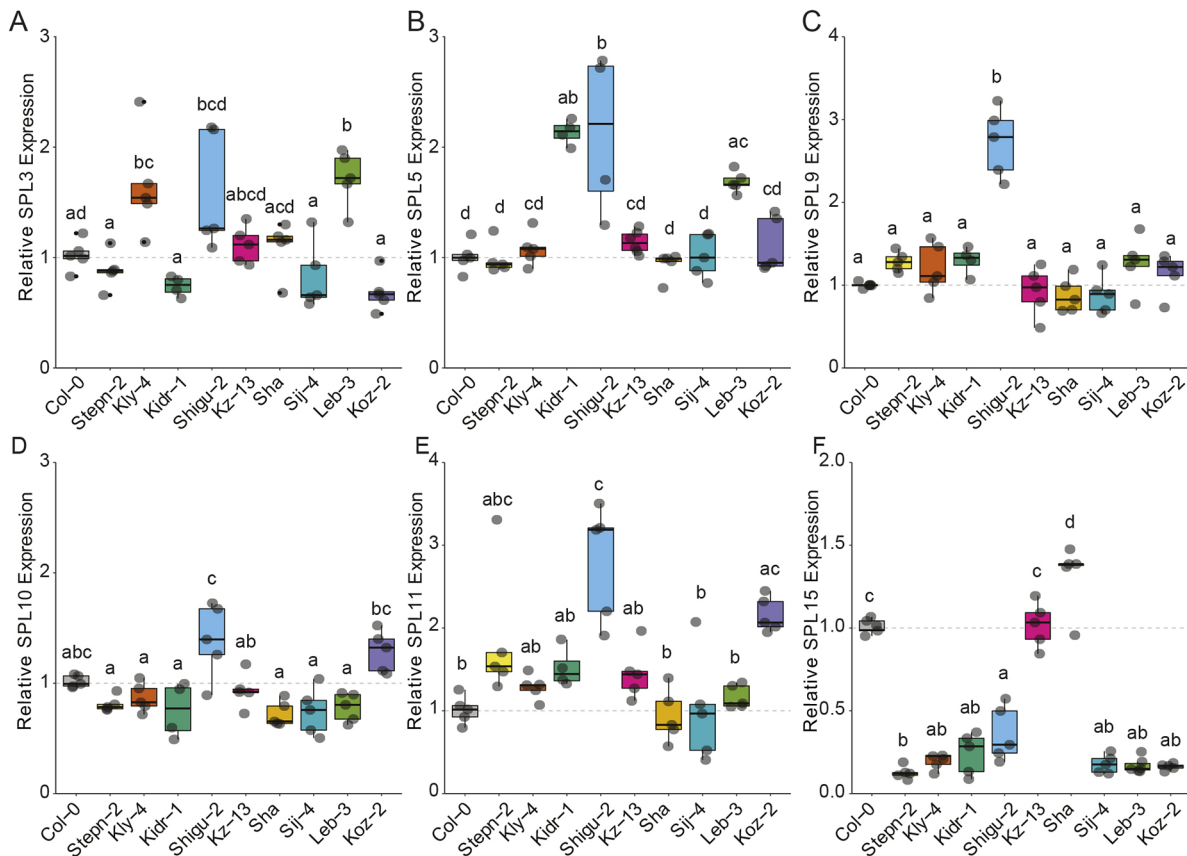


Fig. 5. Relative abundance of SPL transcripts in leaf primordia of early Central Asian accessions. (A-F) The abundance of *SPL3*, *SPL5*, *SPL9*, *SPL10*, *SPL11* and *SPL15* mRNAs relative to *ACT2* in the primordia of leaves 1&2 of Central Asian accessions. Accessions are in the same order as in Fig. 3E ($n=5$). Significantly distinct groups (denoted by letters) were determined by one-way ANOVA followed by Tukey HSD test ($P=0.05$). Gray circles indicate biological replicates; black dots indicate outliers; center line marks the median value; boxes outline the first and third quartiles; whiskers mark minimum and maximum values.

significant QTL on the top of chromosome 5, in a different location from the QTL for leaves lacking abaxial trichomes (Fig. 9C,D). These results indicate that the precocious vegetative development of Sha is controlled by multiple genes, with different loci controlling different aspects of its phenotype.

RILs grown under long days demonstrate that QTLs regulating vegetative phase change and reproductive phase change are distinct in Sha

To determine whether the QTLs that regulate vegetative phase change are independent of the QTLs that regulate flowering time, Sha \times Col-0 RILs were also grown under floral inductive (LD) conditions. Ten plants from each genotype were scored for the time to first open flower and for the number of leaves lacking abaxial trichomes. Under LD conditions, Sha produced significantly fewer leaves without abaxial trichomes (Fig. 10A), but flowered slightly later than Col-0 (Fig. 10C). QTL analysis of the number of leaves lacking abaxial trichomes revealed a QTL at the bottom of chromosome 5, located in the same position as the QTL associated with this trait in SD conditions, as well as less-significant QTLs that resembled those previously detected on chromosome 1 (Fig. 10B). QTL analysis of flowering time, using days to first open flower as the phenotype, revealed two QTLs different from those regulating vegetative phase change. The most significant is located on chromosome 1, and likely corresponds to the flowering time gene *FLOWERING LOCUS T* (*FT*) or *TREHALOSE PHOSPHATE SYNTHASE1* (*TPS1*), a gene involved in sugar metabolism that

impacts flowering (Schwartz et al., 2009; Blázquez et al., 1998; Eastmond et al., 2002; Wahl et al., 2013). *TPS1* has also been shown to impact vegetative phase change (Ponnu et al., 2020). A second QTL located at the top of chromosome 3 may correspond to the flowering time gene *VRN1* (Fig. 10D) (Schwartz et al., 2009). These findings partially reflect QTLs previously found to regulate flowering time in Sha when using RILs derived from Sha and the natural accession Bay-0 (El-Lithy et al., 2004; Symonds et al., 2005; Botto and Coluccio, 2007; Jiménez-Gómez et al., 2010). Importantly, these results indicate that distinct genetic loci regulate flowering time and the timing of vegetative phase change in Sha and Col-0.

Analysis of candidate genes within the Sha \times Col-0 QTLs

To identify candidate genes of interest within the QTLs we found, we used available genomic and transcriptomic data from Sha and Col-0 accessions from the 1001 Genomes database (<https://1001genomes.org/>, <http://signal.salk.edu/1001.php>). We focused on the QTLs on chromosomes 2 and 5, as together they encompassed the largest amount of variance in the RIL population and were independent of the QTLs associated with flowering time. Additionally, the chromosome 2 QTL was found to regulate both appearance of abaxial trichomes and adult leaf shape, and the chromosome 5 QTL was found to regulate abaxial trichomes robustly under both SD and LD conditions, indicating that they both have important roles in regulating vegetative phase change in Sha.

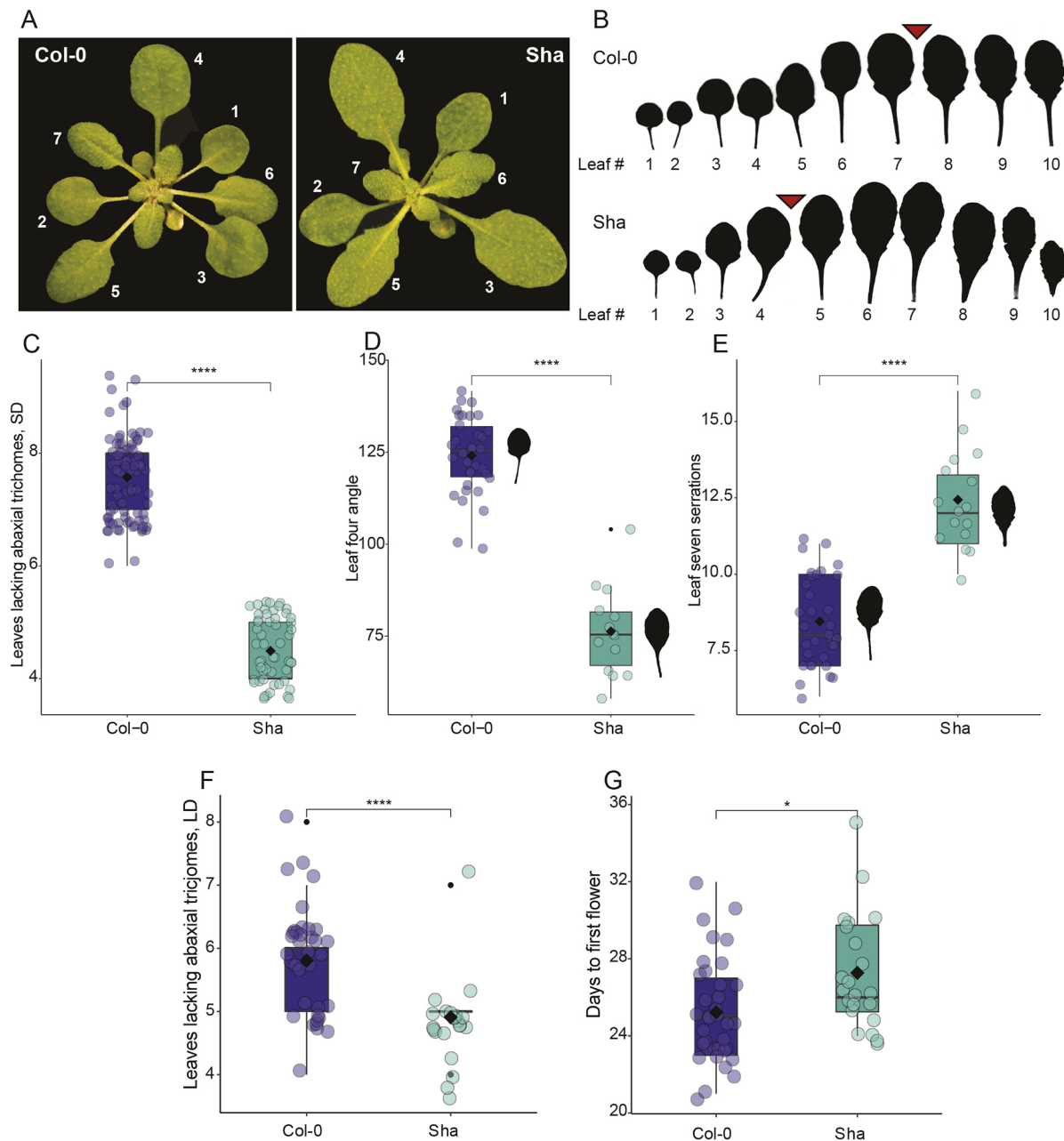


Fig. 6. *Sha* undergoes early vegetative phase change. (A) Four-week-old *Col-0* and *Sha* plants grown in SD. (B) Fully expanded rosette leaves of *Sha* and *Col-0*. Red arrowheads indicate average position of the first leaf producing abaxial trichomes. (C-E) The number of leaves lacking abaxial trichomes (C), the angle of the leaf base of leaf 4 (D) and the number of serrations on the lamina of leaf 7 (E) in *Sha* and *Col-0* grown under SD conditions. Significance was determined by two-tailed Student's *t*-test (**** $P < 0.0001$). Purple and green circles indicate biological replicates; black dots indicate outliers; center line marks the median value; boxes outline the first and third quartiles; whiskers mark minimum and maximum values. (F,G) The number of leaves lacking abaxial trichomes (F) and days to first open flower (G) in *Col-0* and *Sha* grown in LD conditions. Significance was determined by two-tailed Student's *t*-test (* $P < 0.05$, **** $P < 0.0001$). Purple and green circles indicate biological replicates; black dots indicate outliers; center line marks the median value; boxes outline the first and third quartiles; whiskers mark minimum and maximum values.

Using a *de novo* genomic assembly of *Sha* (Jiao and Schneeberger, 2020), and the Tair10 *Col-0* assembly (<https://www.arabidopsis.org/download/>), we identified single nucleotide polymorphisms (SNPs) between *Col-0* and *Sha* within these QTLs, and used the program SnpEff (Cingolani et al., 2012) to predict the impact of these SNPs on the function of the >5000 protein-coding genes within these QTLs (results shown in Table S4). In addition, we used RNA-sequencing data from the 1001 Genomes database (Kawakatsu et al., 2016) to determine which of these genes are

differentially expressed in *Sha* and *Col-0* (results shown in Table S4). These analyses helped inform our assessment of candidate genes for the regulation of vegetative phase change in *Sha*.

In the QTL on chromosome 5, we explored several genes known to be involved in regulation of vegetative phase change. The first was *SPL13*, as it is a known target of miR156 (Xu et al., 2016). We found that *SPL13* abundance was lower in *Sha* than in *Col-0* (Fig. 11A), likely because *Col-0* contains a tandem duplication of

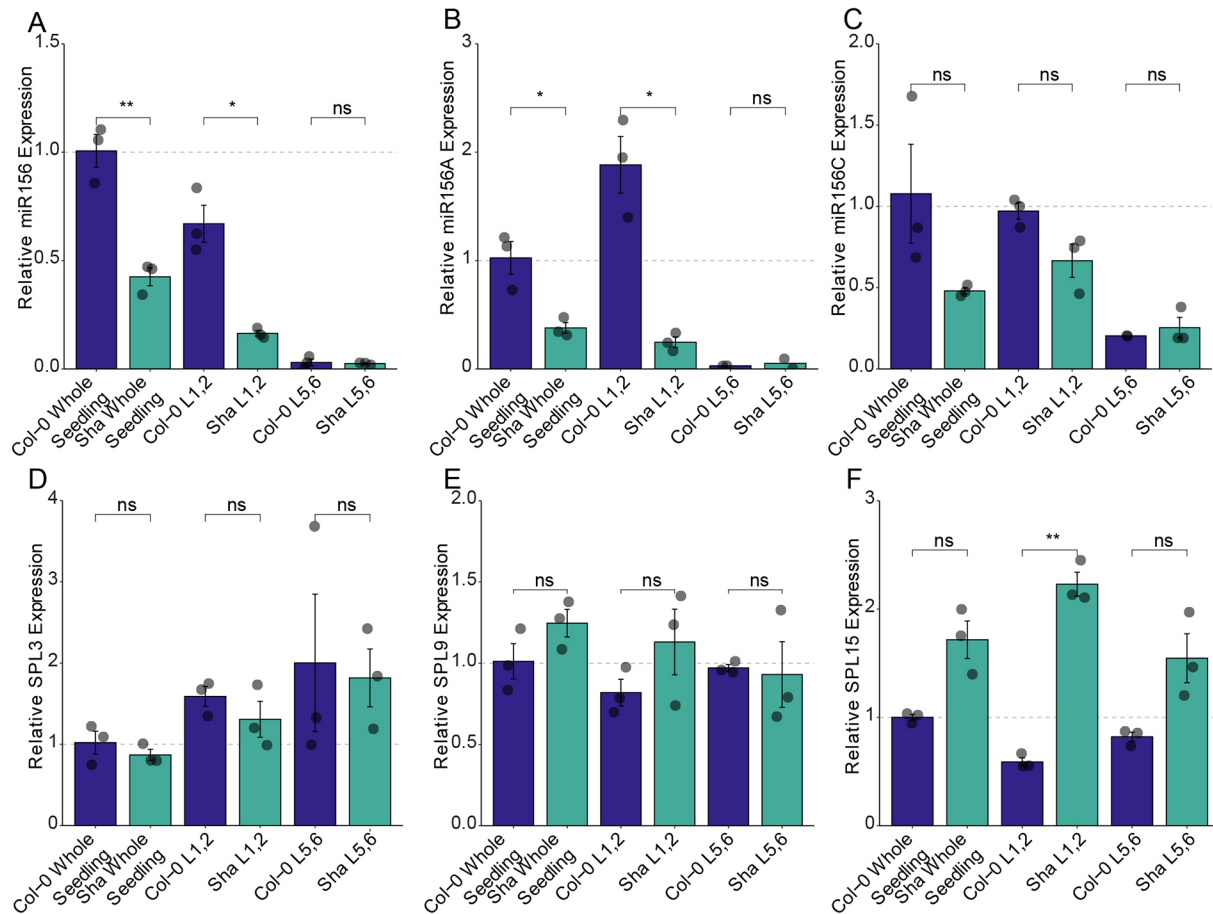


Fig. 7. Relative abundance of miR156 and SPL transcripts in Col-0 and Sha. (A) Mature miR156 abundance relative to Snor101 in seedlings and leaf primordia of Sha and Col-0. Data are presented as mean \pm s.e.m. ($n=3$). Gray circles indicate biological replicates. Significance was determined by two-tailed Student's t -test. (B-F) *pri-miR156A*, *pri-miR156C*, *SPL3*, *SPL9* and *SPL15* mRNA abundance relative to *ACT7* in whole seedling and in leaf primordia of Sha and Col-0. Data are presented as mean \pm s.e.m. ($n=3$). Gray dots indicate biological replicates; black dots indicate outliers. Significance was determined by two-tailed Student's t -test. ns, not significant; * $P<0.05$, ** $P<0.01$.

SPL13 that is absent in Sha (Xu et al., 2016). Two additional genes within this region, *TOE2* and *TOE3*, are known to regulate both abaxial trichome production and flowering time (Wu et al., 2009). These genes are targets of the microRNA miR172, are highly expressed during the juvenile phase, and promote the expression of juvenile traits (Aukerman and Sakai, 2003; Zhu and Helliwell, 2011; Xu et al., 2019). However, the expression of *TOE2* and *TOE3* did not match the pattern expected from the early phase change phenotype of Sha (Fig. 11C,D). Additionally, none of the SNPs in the Sha alleles of these genes is predicted to have a high impact on its own function (Table S4). Consequently, we ruled out *SPL13*, *TOE2* and *TOE3* as candidates.

The QTL on chromosome 2 contained two candidates known to be involved in regulation of phase change: *MIR156A* and *TOE1*. We found that *pri-miR156A* levels were much lower in Sha than in Col-0 across development, which matches what would be expected for the precocious phenotype of Sha (Fig. 7B). *TOE1* is highly expressed in Col-0 during the juvenile phase, and a decrease in its expression promotes adult leaf traits, including abaxial trichome production (Jung et al., 2014; Wang et al., 2019). We found that *TOE1* is expressed at a much lower level in Sha than in Col-0 (Fig. 11B, Table S4), which is consistent with its early vegetative phase change phenotype. Moreover, three SNPs within the coding region of *TOE1* are predicted to have a high impact on gene function, and an

additional seven SNPs are predicted to have a moderate to low impact on gene function (Table S4). Together, these data indicate that *TOE1* and *MIR156A* are candidates for the QTL on chromosome 2.

DISCUSSION

Juvenile and adult vegetative traits impact plant fitness, and the genetic module that mediates the transition between these phases – miR156/miR157 and their SPL targets – is conserved across land plants (Axtell and Bowman, 2008; Cui et al., 2014; Lawrence et al., 2021; Leichty and Poethig, 2019; Wang and Wang, 2015). These observations indicate that vegetative phase change is an important developmental transition in plants and suggest that an understanding of its genetic architecture will provide insights into both the adaptive significance and molecular mechanism of this transition. Several studies have characterized phenotypic variation in timing of vegetative phase change in natural populations of plants, but few have determined the genetic basis or the adaptive significance of this variation (Wiltshire et al., 1998; Jordan et al., 2000; Foerster et al., 2015). To address these questions, we characterized the timing of vegetative phase change in natural accessions of *A. thaliana*, examined the relationships between leaf development, reproductive development, climate and the miR156/SPL pathway, and mapped QTLs affecting phase-specific traits.

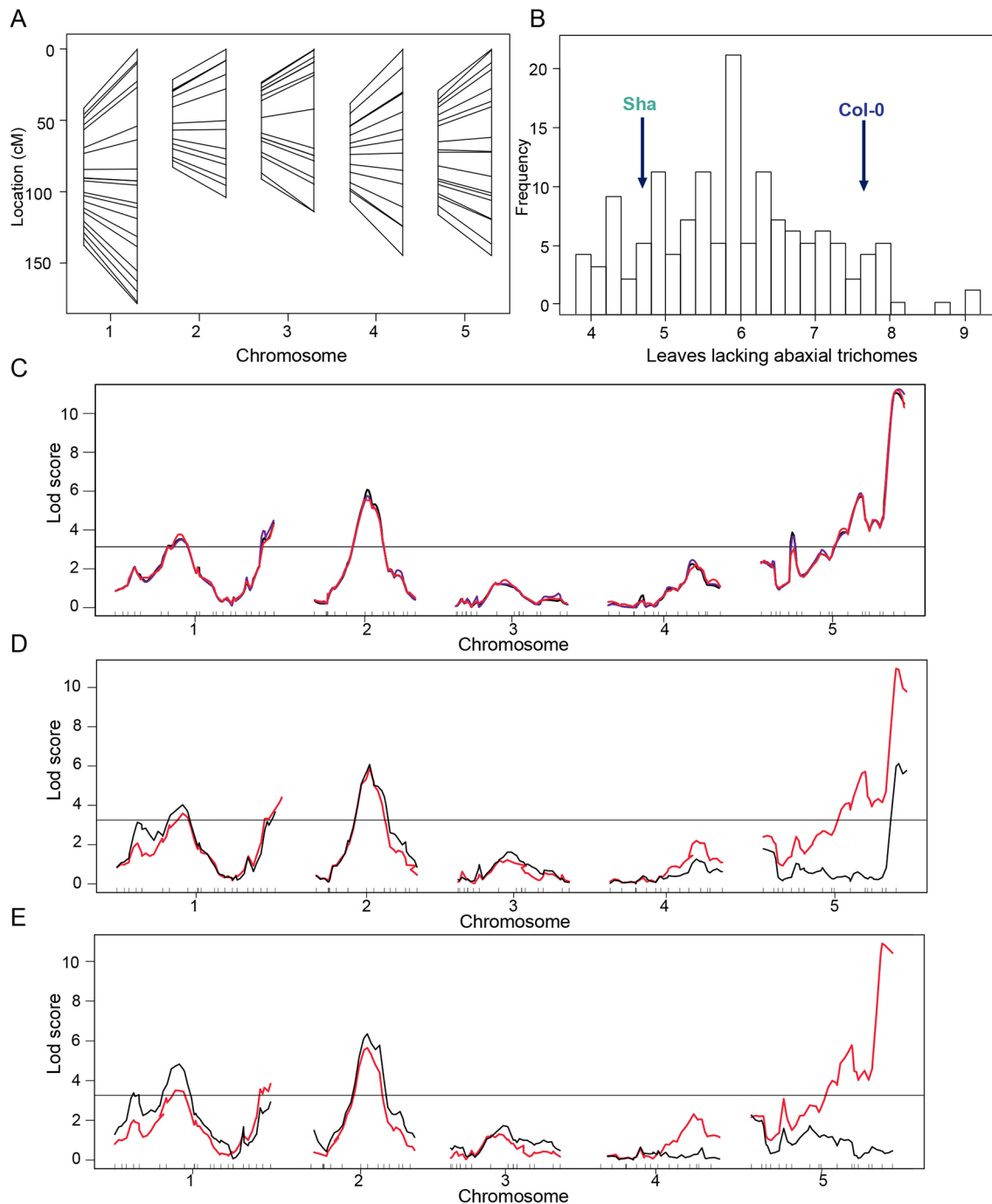


Fig. 8. QTL mapping of the number of leaves lacking abaxial trichomes in Sha×Col-0 RILs in SD conditions. (A) Location of molecular markers on the recombination (left vertical line) and physical (right vertical line) maps in Sha×Col-0 RILs. (B) Phenotypic distribution of the number of leaves lacking axial trichomes of 164 Sha×Col-0 RILs grown in SD conditions. Arrows indicate the average phenotype of Col-0 and Sha parents. (C) QTL analysis for the number of leaves lacking abaxial trichomes with a LOD score threshold of 3.2 (horizontal black line) based on 1000 permutations and 95% significance. Black lines indicate the LOD score based on maximum likelihood via the EM algorithm, blue lines indicate Haley–Knott regression, red lines indicate multiple imputation method. (D,E) Covariate analysis using the peak coordinates of the QTLs on chromosome 5. Red lines are LOD scores based on leaves lacking abaxial trichomes using maximum likelihood method via the EM algorithm. Black lines are LOD scores based on a genome scan for number of leaves lacking abaxial trichomes with the effects of each QTL peak on chromosome 5 incorporated as an interacting covariate.

Unexpectedly, we found that traits associated with transition to the adult phase, such as appearance of abaxial trichomes and a narrow, serrated leaf shape, were decoupled in many of the natural accessions we studied, including half of the precocious Central Asian accessions. Additionally, we found that the genetic architecture underlying traits were different in the accession Sha,

with both shared and distinct QTLs regulating leaf shape, serrations and abaxial trichome development. A similar phenomenon has been observed in swollen-thorn acacias, in which different components of the swollen-thorn syndrome are expressed in slightly different temporal patterns in different accessions (Leichty and Poethig, 2019). This result suggests that the temporal expression pattern of

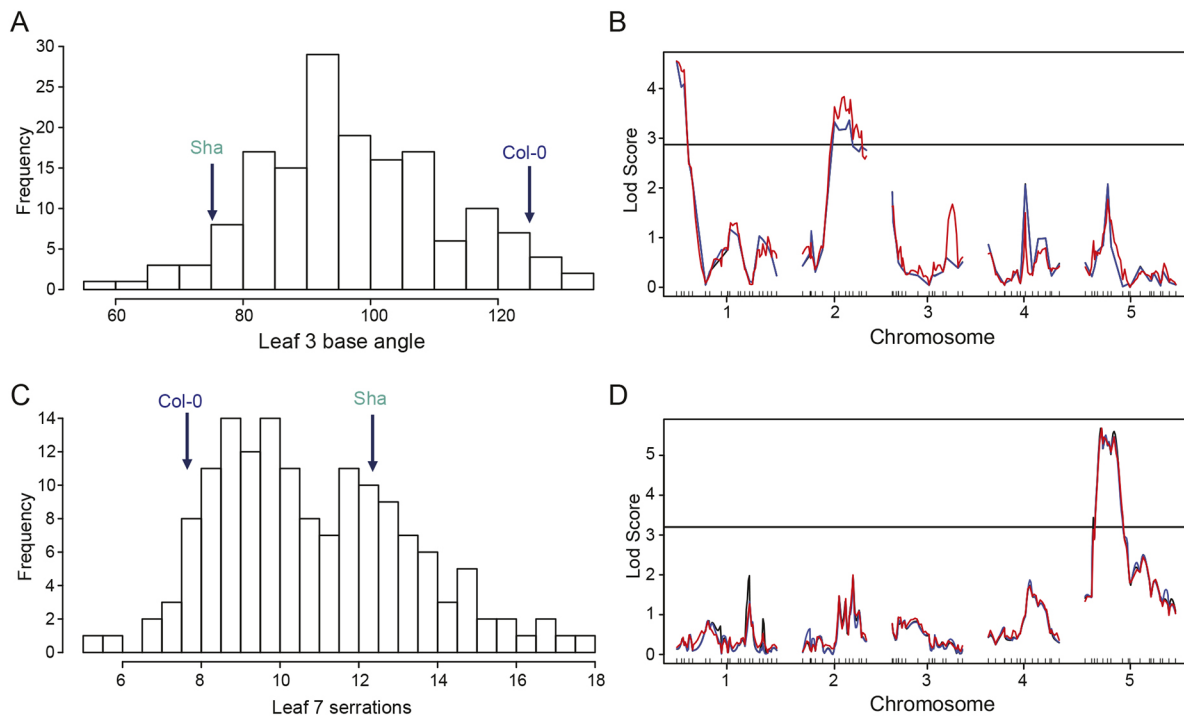


Fig. 9. QTL mapping of leaf shape in Sha×Col-0 RILs in SD conditions. (A) Phenotypic distribution in leaf 3 base angle of 164 Sha×Col-0 RILs grown in SD conditions. Arrows indicate the average phenotype of Col-0 and Sha parents. (B) QTL analysis for leaf 3 base angle with a LOD score threshold of 2.91 (horizontal black line) based on 1000 permutations and 95% significance. Black lines indicate the LOD score based on maximum likelihood via the EM algorithm, blue lines indicate Haley–Knott regression, red lines indicate multiple imputation method. (C) Phenotypic distribution in number of serrations on leaf 7 of 164 Sha×Col-0 RILs grown in SD conditions. Arrows indicate the average phenotype of Col-0 and Sha parents. (D) QTL analysis for number of serrations on leaf 7 in SD conditions with a LOD score threshold of 3.07 based on 1000 permutations and 95% significance. Black lines are the LOD score based on maximum likelihood via the EM algorithm, blue lines are Haley–Knott regression, red lines are multiple imputation method.

each trait is regulated by genes specific to each trait, as well as by miR156.

The dissociation of different phase-specific traits may be functionally significant, as trichomes are typically associated with defense against herbivory (Duffey, 1986; Dalin et al., 2008), whereas leaf shape is associated with adaptation to temperature and water availability (Givnish, 1979; Greenwood, 2005). Variation in leaf developmental traits may therefore be promoted by varying environmental challenges. This hypothesis is supported by our finding that seasonal and annual variation in temperature in Central Asia is associated with early development of adult leaf shape, but not production of abaxial trichomes. It also agrees with literature in other species, such as *Eucalyptus* and *Acacia*, showing that dry and wet climates are associated with variation in the timing of vegetative phase change (Jordan et al., 2000; Rose et al., 2019).

Consistent with the hypothesis that genes that regulate certain phase-specific traits play an important role in vegetative phase change, we found that miR156 and SPL gene expression was not necessarily correlated with the phenotypic variation we observed. Furthermore, QTL analysis of the basis for the early phase change phenotype of Sha revealed eight QTLs associated with phase-specific traits, only one of which potentially corresponds to a gene encoding miR156. A variety of factors impact the transcription of SPL genes independently of miR156, including low light intensity (Xu et al., 2021), photoperiod (Jung et al., 2012) and epigenetic repression by the POLYCOMB REPRESSIVE COMPLEX 1 (Picó et al., 2015; Li et al., 2017). Additionally, the microRNA miR172 regulates abaxial trichome production via its effect on *TOE* gene expression (Huijser and Schmid, 2011; Wang et al., 2019; Wu et al., 2009; Xu et al., 2019). Any combination of these mechanisms could

be responsible for the lack of complete coordination between the timing of vegetative phase change and the level of miR156 expression. Unfortunately, it is difficult to interpret the functional significance of variation in the abundance of miR156 or SPL transcripts because miR156 regulates SPL expression primarily through translational repression. Very small differences in miR156 abundance can have dramatic effects on the level of SPL proteins while having little to no effect on the abundance of SPL transcripts (He et al., 2018a). This complicates comparisons between accessions because the absence of an apparent difference in miR156 or SPL transcript abundance does not necessarily mean that SPL protein levels are the same in these accessions.

Although vegetative phase change is often thought to be linked to reproductive competence (Wang et al., 2009; Wang, 2014; Xie et al., 2020), we observed no correlation between adult leaf base angle and reproductive traits (days to first open flower) in non-inductive conditions. We found additional evidence of this in a comparison of these traits in a worldwide sample of natural accessions and from an analysis of RILs derived from a cross between Col-0 and Sha. The lack of correlation suggests that these developmental transitions are not intimately linked and indicates that they likely respond differently to natural selection.

We did, however, find that abaxial trichome production was slightly correlated with time to first open flower in floral inductive LD conditions. We suspect this is because abaxial trichome production is at least partly regulated by the *TOE1*/miR172 pathway (Wang et al., 2019), which also plays a role in flowering time (Aukerman and Sakai, 2003). The flowering gene *FLC* also controls certain vegetative traits (Willmann and Poethig, 2011) and represses *SPL15* expression (Deng et al., 2011). However, we do not

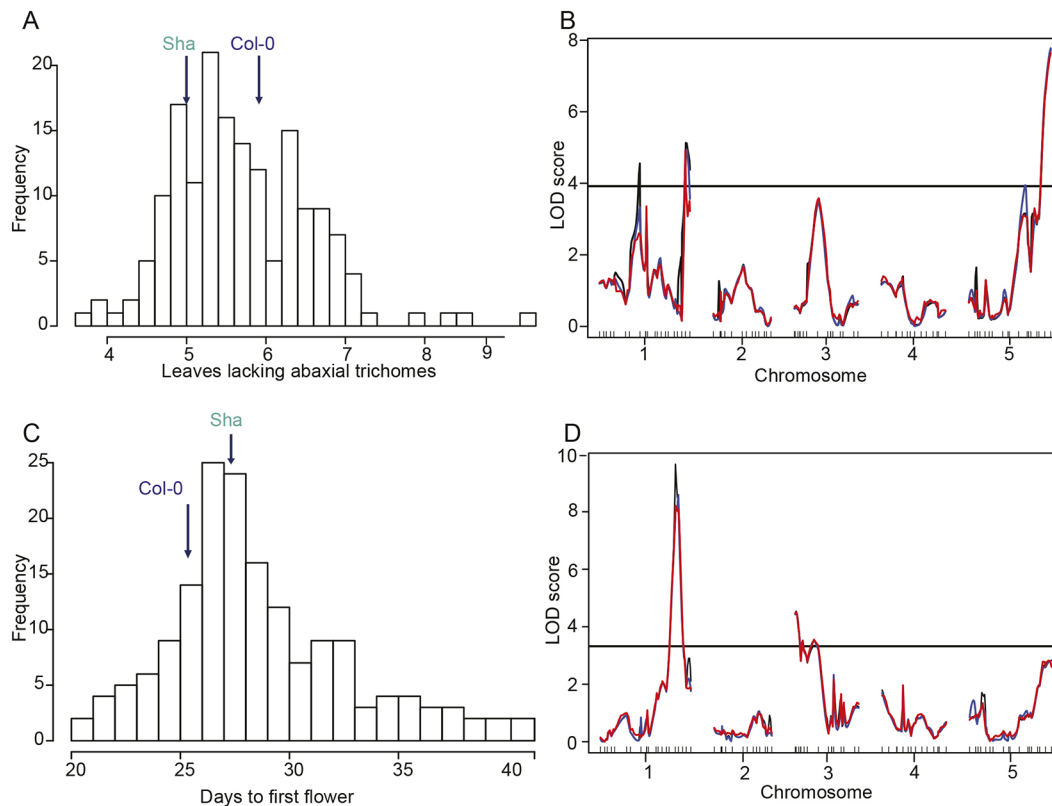


Fig. 10. QTL analysis of days to first flower in Sha×Col-0 RILs in LD conditions. (A) Phenotypic distribution in the number of leaves lacking abaxial trichomes of 164 Sha×Col-0 RILs grown in LD conditions. Arrows indicate the average phenotype of Col-0 and Sha parents. (B) QTL analysis for the number of leaves lacking abaxial trichomes grown in LD conditions with a LOD score threshold of 3.92 (horizontal black line) based on 1000 permutations and 95% significance. Black lines are the LOD score based on maximum likelihood via the EM algorithm, blue lines are Haley–Knott regression, red lines are multiple imputation method. (C) Phenotypic distribution in the number of days to first open flower of 164 Sha×Col-0 RILs grown in LD conditions. Arrows indicate the average phenotype of Col-0 and Sha parents. (D) QTL analysis for days to first open flower grown in LD conditions. LOD score threshold is 3.31 based on 1000 permutations and 95% significance. Black lines are the LOD score based on maximum likelihood via the EM algorithm, blue lines are Haley–Knott regression, red lines are multiple imputation method.

think that *FLC* can explain the differences we observed because accessions were vernalized for 4 weeks, which effectively reduces the effect of *FRI/FLC* on flowering time (Sheldon et al., 2000). Additionally, we found that the differences in the timing of vegetative phase change in different accessions persisted even when flowering time was manipulated through vernalization. This key result indicates that vegetative phase change is largely independent of reproductive phase change (i.e. floral induction). It is true that all of the accessions we examined only flowered when they were in the adult phase. Although this could mean that vegetative phase change is necessary for flowering even if it does not directly lead to floral induction, this is unlikely (at least in *A. thaliana*) because constitutive overexpression of *miR156* in Col-0 has only a minor effect on flowering time (Xu et al., 2016). The conclusion that vegetative phase change and flowering are largely unrelated is also supported by previous studies, which showed that SD conditions produce a very large delay in flowering time (greater than 30 days), but produce only a small delay (2 days) in vegetative phase change (Willmann and Poethig, 2011; Xu et al., 2016). An alternative possibility is that vegetative phase change and floral induction are regulated in parallel by the same factors and thus change in a coordinated, but not sequentially dependent, fashion.

Further work is necessary to identify the genes responsible for natural variation in the timing of vegetative phase change in *A. thaliana*. We expect that these studies will reveal new and functionally interesting alleles of genes known to have a role in

vegetative phase change, and uncover genes involved in the regulation of this important developmental transition.

MATERIALS AND METHODS

Data availability

All ABRC stock numbers, geographic data and phenotypic data of natural accessions used in this study are available in Table S1. Sha×Col-0 recombinant inbred lines are available from the Versailles Stock Center at <http://publiclines.versailles.inrae.fr/rils/index> and genotypic data for these lines is available at <http://publiclines.versailles.inrae.fr/page/13>. All phenotypic and genotypic data used for QTL mapping are given in Table S2. All primers used in this study are listed in Table S3. Results from SnpEff and DeSeq of candidate genes are given in Table S4.

Plant material and growth conditions

Stocks of natural accessions were obtained from the *Arabidopsis* Biological Resource Center (ABRC, Ohio State University, OH, USA) and corresponding geographic data was obtained from the 1001 Genomes database (Alonso-Blanco et al., 2016). ABRC stock numbers of these accessions and geographic coordinates of their collection locations and phenotypic data are given in Table S1.

Seeds were sown on Farfard #2 soil (Farfard) treated with fertilizer (Peters Peat Lite 15-16-17), Marathon 1% granular (Marathon) and Scanmask Spray (Biologic) for insect control and kept at 4°C for 2 days (non-vernalized) or 4 weeks (vernalized). They were then transferred to a growth chamber, with the transfer day counted as the planting date. Plants were grown at 22°C under a combination of cool white and Gro LITE fluorescent bulbs (Interlectric, F32T8/GL/WS) in either LD (16 h light/8 h dark;

100 $\mu\text{mol m}^{-2} \text{s}^{-1}$) or SD (10 h light/14 h dark; 130 $\mu\text{mol m}^{-2} \text{s}^{-1}$) conditions. Unless indicated otherwise, all experiments in SD and LD conditions were conducted with plants vernalized for 4 weeks. In experiments with numerous flats, seeds of each genotype were dispersed into multiple groups across flats, and flats were rotated in the growth chambers every 3 days to facilitate even distribution of light throughout the experiment. There was no statistical difference between the phenotype of Col-0 plants grown in each flat (two-tailed Student's *t*-test), allowing for pooling of data between flats.

For QTL mapping, the 13RV Core-pop set derived from Sha and Col-0 accessions was obtained from the Versailles *Arabidopsis* Stock Center (Simon et al., 2008; <http://publiclines.versailles.inrae.fr/rils/index>). From each of these 164 lines, plus the Sha and Col-0 parental lines, 10–12 individuals were grown as described above in both LD and SD conditions and scored for number of leaves lacking abaxial trichomes (both SD and LD), leaf 3 base angle (both LD and SD), leaf 7 serrations (SD only) and days to first open flower (LD only). There was no statistical difference between the phenotype of Col-0 or Sha plants grown in each flat (two-tailed Student's *t*-test), allowing for pooling of data between flats. All phenotypic and genotypic data used for QTL mapping are given in Table S2.

Leaf shape and phenotypic measurements

The presence of trichomes on the abaxial side of the lamina was determined with the aid of a dissecting microscope by gently lifting the leaves of soil-grown plants. Flowering time was measured by the number of days to the appearance of petals in the bud of the first flower; bolting time was defined by days until bolt reached 3 cm, and total rosette leaf number was counted as the number of rosette leaves. To analyze leaf shape, fully expanded leaves were attached to paper using double-sided tape and scanned. The angle of the leaf base corresponds to the angle between two lines tangent to the base of the lamina intersecting at the petiole and was measured using Fiji (Fig. S1A) (Schindelin et al., 2012). We measured leaf 3 in RILs, and leaf 4 in natural accessions. To measure the appearance of leaf serrations, the number of serrations on leaf 7 was counted using the leaf shape analysis program Lamina (Bylesjö et al., 2008). In all cases, at least 6–12 plants of each genotype were measured.

PCA of climatic variables

Collection locations (longitude and latitude) of the 70 accessions used in this study were obtained from the 1001 Genomes database (<https://1001genomes.org/accessions.html>). Climate data, which included 19 bioclimatic variables and altitude for each of these locations, were extracted from the WorldClim Database with 30 arc-second spatial resolution (<http://www.worldclim.org/current>; Fick and Hijmans, 2017). PCA was performed in R with the `prcomp(center and scale=TRUE)` function using the data for these 20 climatic variables. Data are available in Table S1.

Measuring miRNA and mRNA abundance by RT-qPCR

Tissue from whole 2-week-old seedlings and leaf primordia 2 mm in length was collected in biological replicates and ground in liquid nitrogen. Total RNA was extracted using Trizol (Invitrogen) and treated with RNase-free DNase (Qiagen) as per the manufacturer's instructions and 300 ng of total RNA was used for reverse transcription using Superscript III First Strand Synthesis System (Invitrogen). RT-PCR for smRNAs was carried out using primers specific for mature sequences of miR156 in combination with the stem-loop RT primers described by Varkonyi-Gasic et al. (2007) and a reverse primer specific to SnoR101 (Xu et al., 2015). For mRNA RT-PCR amplification, we used a polyT primer. The resulting cDNA was quantified by qPCR using a three-step amplification protocol and SYBR-Green Master Mix (Bimake) in technical triplicates with primers specific to each mRNA or miRNA using either SnoR101 (miRNA) or *ACT2* (mRNA) as the endogenous controls. All primers used are listed in Table S3. Relative abundance was calculated using the $2^{-\Delta\Delta C_t}$ method (Livak and Schmittgen, 2001). The data presented represent the averages of three to five biological replicates, as indicated for each figure.

QTL analysis

QTL interval mapping was implemented in the R/qtl package (Broman et al., 2003) in R (<https://www.r-project.org/>) using phenotypic data from Sha \times Col-0 RILs (Table S2). Logarithm of the odds (LOD) scores for each phenotype were computed via the 'scanone' function based on maximum likelihood via the expectation-maximization (EM) algorithm (black lines), Haley-Knott regression (blue lines), and the multiple imputation method (red lines) (Churchill and Doerge, 1994; Sen and Churchill, 2001). The experiment-wide 0.05 significance LOD score threshold was determined for each trait from 1000 permutations. Analysis of epistasis for each QTL was performed using the multiple imputation method by including the location of the QTL peak as a covariate to the trait of interest. In short, the 'scanone' function was used to scan the genome for associations while controlling for the marker location nearest to each peak as an interacting covariate. For more detail, see <https://rql.org/rqtltour.pdf> and Broman and Sen (2009).

SnpEff

Genomic sequences and annotation files of the Tair10 Col-0 assembly (<https://www.arabidopsis.org/download/>) and the 1001 Genome Project Sha assembly (<https://1001genomes.org/data/MPIPZ/MPIPZJiao2020>; Jiao and Schneeberger, 2020) were used for analysis.

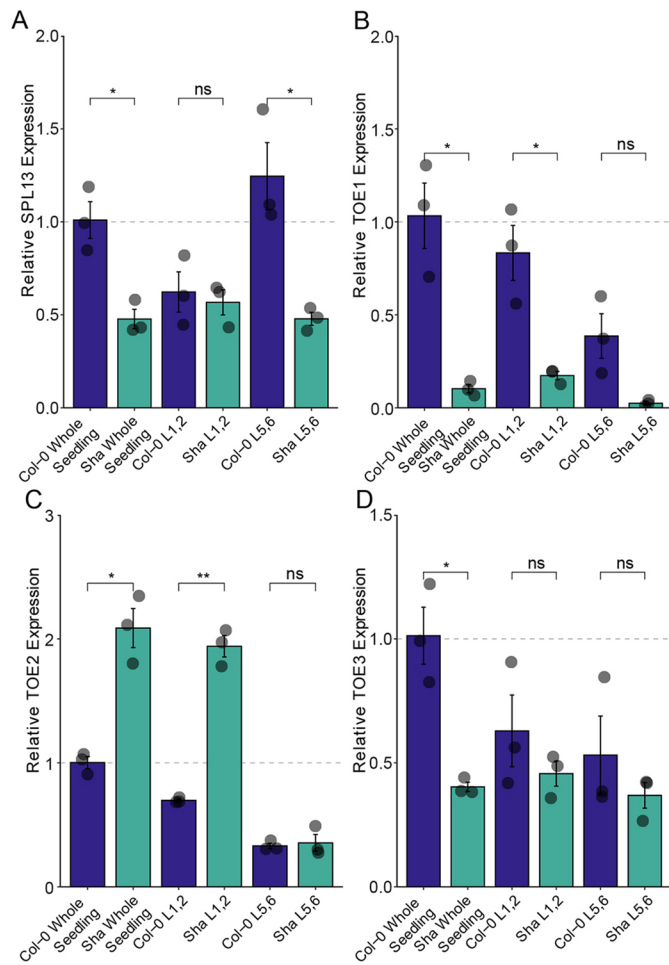


Fig. 11. Analysis of candidate genes within significant QTLs on chromosomes 2 and 5. (A–D) RT-qPCR analysis of *SPL13*, *TOE1*, *TOE2* and *TOE3* mRNA abundance relative to *ACT2* in whole seedlings and leaf primordia of Sha and Col-0. Data are presented as mean \pm s.e.m. ($n=3$). Gray circles indicate biological replicates, black dots indicate outliers. Significance was determined by two-tailed Student's *t*-test (ns, not significant; * $P<0.05$, ** $P<0.01$).

Col-0 and Sha whole-genome sequences were aligned and visualized using Mauve alignment software (Darling et al., 2004). Homologous regions from the Sha and Col-0 genomes that corresponded to the RIL genomic markers closest to boundaries of each QTL were extracted for further analysis. Chromosome 2 coordinates used were 7650461-13471565 and 7424367-13257809 for Col-0 and Sha, respectively. Chromosome 5 coordinates used for analysis were 16368385-27316966 and 16482000-27639917 for Col-0 and Sha, respectively. The resulting sequences were aligned using MAFFT (Katoh, 2002) and converted to variant call format (VCF) files (Lindenbaum, 2015) using Col-0 (Tair10) as the reference sequence. The predicted effects of SNPs on gene function within the QTL regions on chromosomes 2 and 5 were then predicted with SnpEff (Cingolani et al., 2012). Results are shown in Table S4.

Differential gene expression

Transcription data from leaf tissue were obtained from the 1001 Epigenomes database (<http://neomorph.salk.edu/1001.php>) for samples Col-0 (Sample 6909, Gene Expression Omnibus accession number GSM2136441) and Sha (Sample 10015, Gene Expression Omnibus accession number GSM2135725) (Kawakatsu et al., 2016). Normalized data were filtered to select for genes within each QTL region (same as above) and differential expression was determined using the DeSeq2 package (Love et al., 2014) in R. Results are shown in Table S4.

Statistical analysis

All statistical tests and analyses were conducted in R version 3.6.1. Linear regression was carried out with the `lm()` function. Two-tailed Student's *t*-test was performed using the `stat_compare_means(method="t.test")` function as part of the library (`ggpubr`) package. ANOVA was carried out using the `aov(model)` function and a linear model (`lm()` function) between variables. Tukey Honest Significant Differences (HSD) test was applied to each pair of treatments using the `TukeyHSD(conf.level=0.95)` function.

Acknowledgements

We thank the *Arabidopsis* Biological Resource Center and Versailles Stock Center for seed stocks, Bishwas Sharma for technical assistance, and members of the Poethig lab for helpful discussions. We also thank three anonymous reviewers whose feedback helped to improve and clarify the manuscript.

Competing interests

The authors declare no competing or financial interests.

Author contributions

Conceptualization: E.D., J.H.; Methodology: E.D.; Validation: E.D.; Formal analysis: E.D., Y.Z., R.S.P.; Investigation: E.D.; Data curation: E.D., Y.Z.; Writing - original draft: E.D.; Writing - review & editing: E.D., J.H., R.S.P.; Supervision: R.S.P.; Project administration: R.S.P.; Funding acquisition: E.D., R.S.P.

Funding

This research was funded by the National Institutes of Health (HD083185 to E.D. and GM051893 to R.S.P. Deposited in PMC for release after 12 months.

Peer review history

The peer review history is available online at <https://journals.biologists.com/dev/article-lookup/doi/10.1242/dev.200321>.

References

Allsopp, A. (1967). Heteroblastic development in vascular plants. In *Advances in Morphogenesis* (ed. M. Abercrombie and J. Brachet), pp. 127-171. Elsevier.

Aloni, R. (2021). Regulation of juvenile-adult transition and rejuvenations. In *Vascular Differentiation and Plant Hormones* (ed. R. Aloni), pp. 215-222. Cham: Springer International Publishing.

Alonso-Blanco, C., El-Assal, S. E.-D., Coupland, G. and Koornneef, M. (1998). Analysis of natural allelic variation at flowering time loci in the Landsberg erecta and Cape Verde Islands ecotypes of *Arabidopsis thaliana*. *Genetics* **149**, 749-764. doi:10.1093/genetics/149.2.749

Alonso-Blanco, C., Andrade, J., Becker, C., Bemm, F., Bergelson, J., Borgwardt, K. M., Cao, J., Chae, E., Dezaan, T. M., Ding, W. et al. (2016). 1,135 genomes reveal the global pattern of polymorphism in *Arabidopsis thaliana*. *Cell* **166**, 481-491. doi:10.1016/j.cell.2016.05.063

Amasino, R. (2010). Seasonal and developmental timing of flowering. *Plant J.* **61**, 1001-1013. doi:10.1111/j.1365-313X.2010.04148.x

Andrés, F. and Coupland, G. (2012). The genetic basis of flowering responses to seasonal cues. *Nat. Rev. Genet.* **13**, 627-639. doi:10.1038/nrg3291

Aukerman, M. J. and Sakai, H. (2003). Regulation of flowering time and floral organ identity by a microRNA and its APETALA2-like target genes. *Plant Cell* **15**, 2730-2741. doi:10.1105/tpc.016238

Axtell, M. J. and Bowman, J. L. (2008). Evolution of plant microRNAs and their targets. *Trends Plant Sci.* **13**, 343-349. doi:10.1016/j.tplants.2008.03.009

Bergelson, J. and Roux, F. (2010). Towards identifying genes underlying ecologically relevant traits in *Arabidopsis thaliana*. *Nat. Rev. Genet.* **11**, 867-879. doi:10.1038/nrg2896

Blázquez, M. A., Santos, E., Flores, C., Martínez-Zapater, J. M., Salinas, J. and Gancedo, C. (1998). Isolation and molecular characterization of the *Arabidopsis TPS1* gene, encoding trehalose-6-phosphate synthase. *Plant J.* **13**, 685-689. doi:10.1046/j.1365-313X.1998.00063.x

Boege, K. and Marquis, R. J. (2005). Facing herbivory as you grow up: the ontogeny of resistance in plants. *Trends Ecol. Evol.* **20**, 441-448. doi:10.1016/j.tree.2005.05.001

Botto, J. F. and Coluccio, M. P. (2007). Seasonal and plant-density dependency for quantitative trait loci affecting flowering time in multiple populations of *Arabidopsis thaliana*. *Plant Cell Environ.* **30**, 1465-1479. doi:10.1111/j.1365-3040.2007.01722.x

Broman, K. W. and Sen, S. (2009). Introduction. In *A Guide to QTL Mapping with R/qtl* (ed. K. W. Broman and S. Sen), pp. 1-20. New York, NY: Springer New York.

Broman, K. W., Wu, H., Sen, S. and Churchill, G. A. (2003). R/qtl: QTL mapping in experimental crosses. *Bioinformatics* **19**, 889-890. doi:10.1093/bioinformatics/btg112

Bylesjö, M., Segura, V., Soolanayakanahally, R. Y., Rae, A. M., Trygg, J., Gustafsson, P., Jansson, S. and Street, N. R. (2008). LAMINA: a tool for rapid quantification of leaf size and shape parameters. *BMC Plant Biol.* **8**, 82. doi:10.1186/1471-2229-8-82

Chen, X. (2004). A MicroRNA as a translational repressor of APETALA2 in *Arabidopsis* flower development. *Science* **303**, 2022-2025. doi:10.1126/science.1088060

Chiang, G. C. K., Barua, D., Kramer, E. M., Amasino, R. M. and Donohue, K. (2009). Major flowering time gene, *FLOWERING LOCUS C*, regulates seed germination in *Arabidopsis thaliana*. *Proc. Natl. Acad. Sci. USA* **106**, 11661-11666. doi:10.1073/pnas.0901367106

Churchill, G. A. and Doerge, R. W. (1994). Empirical threshold values for quantitative trait mapping. *Genetics* **138**, 963-971. doi:10.1093/genetics/138.3.963

Cingolani, P., Platts, A., Wang, L. L., Coon, M., Nguyen, T., Wang, L., Land, S. J., Lu, X. and Ruden, D. M. (2012). A program for annotating and predicting the effects of single nucleotide polymorphisms, SnpEff: SNPs in the genome of *Drosophila melanogaster* strain *w¹¹¹⁸*; iso-2; iso-3. *Fly (Austin)* **6**, 80-92. doi:10.4161/fly.19695

Conway, L. J. and Poethig, R. S. (1993). Heterochrony in plant development. *Semin. Dev. Biol.* **4**, 65-72. doi:10.1006/semb.1993.1008

Cui, L.-G., Shan, J.-X., Shi, M., Gao, J.-P. and Lin, H.-X. (2014). The miR156-SPL9-DFR pathway coordinates the relationship between development and abiotic stress tolerance in plants. *Plant J.* **80**, 1108-1117. doi:10.1111/tpj.12712

Dalin, P., Ågren, J., Björkman, C., Huttunen, P. and Kärkkäinen, K. (2008). Leaf trichome formation and plant resistance to herbivory. In *Induced Plant Resistance to Herbivory* (ed. A. Schaller), pp. 89-105. Dordrecht: Springer Netherlands.

Darling, A. C. E., Mau, B., Blattner, F. R. and Perna, N. T. (2004). Mauve: multiple alignment of conserved genomic sequence with rearrangements. *Genome Res.* **14**, 1394-1403. doi:10.1101/gr.2289704

Deng, W., Ying, H., Helliwell, C. A., Taylor, J. M., Peacock, W. J. and Dennis, E. S. (2011). *FLOWERING LOCUS C (FLC)* regulates development pathways throughout the life cycle of *Arabidopsis*. *Proc. Natl. Acad. Sci. USA* **108**, 6680-6685. doi:10.1073/pnas.1103175108

Duffey, S. S. (1986). Plant glandular trichomes: their partial role in defence against insects. In *Insects Plant Surf* (ed. B. Juniper and S. R. Southwood), pp. 151-172. London: Edward Arnold.

Eastmond, P. J., Van Dijken, A. J. H., Spielman, M., Kerr, A., Tissier, A. F., Dickinson, H. G., Jones, J. D. G., Smeekens, S. C. and Graham, I. A. (2002). Trehalose-6-phosphate synthase 1, which catalyses the first step in trehalose synthesis, is essential for *Arabidopsis* embryo maturation. *Plant J.* **29**, 225-235. doi:10.1046/j.1365-313x.2002.01220.x

El-Lithy, M. E., Clercx, E. J. M., Ruys, G. J., Koornneef, M. and Vreugdenhil, D. (2004). Quantitative trait locus analysis of growth-related traits in a new *Arabidopsis* recombinant inbred population. *Plant Physiol.* **135**, 444-458. doi:10.1104/pp.103.036822

Fick, S. E. and Hijmans, R. J. (2017). WorldClim 2: new 1-km spatial resolution climate surfaces for global land areas. *Int. J. Climatol.* **37**, 4302-4315. doi:10.1002/joc.5086

Foerster, J. M., Beissinger, T., de Leon, N. and Kaepler, S. (2015). Large effect QTL explain natural phenotypic variation for the developmental timing of

- vegetative phase change in maize (*Zea mays* L.). *Theor. Appl. Genet.* **128**, 529-538. doi:10.1007/s00122-014-2451-3
- Gazzani, S., Gendall, A. R., Lister, C. and Dean, C.** (2003). Analysis of the molecular basis of flowering time variation in *Arabidopsis* accessions. *Plant Physiol.* **132**, 1107-1114. doi:10.1104/pp.103.021212
- Givnish, T.** (1979). On the adaptive significance of leaf form. In *Topics in Plant Population Biology* (ed. O. T. Solbrig, S. Jain, G. B. Johnson and P. H. Raven), pp. 375-407. London: Macmillan Education UK.
- Goebel, K.** (1900). *Organography of Plants: Especially the Archegoniatae and Spermaphyta*. Oxford: Clarendon Press.
- González, R., Butković, A., Rivarez, M. P. S. and Elena, S. F.** (2020). Natural variation in *Arabidopsis thaliana* rosette area unveils new genes involved in plant development. *Sci. Rep.* **10**, 17600. doi:10.1038/s41598-020-74723-4
- Greenwood, D. R.** (2005). Leaf form and the reconstruction of past climates. *New Phytol.* **166**, 355-357. doi:10.1111/j.1469-8137.2005.01380.x
- Hackett, W. P.** (1985). Juvenility, maturation, and rejuvenation in woody plants. In *Horticultural Reviews* (ed. J. Janick), pp. 109-155. John Wiley & Sons, Ltd.
- He, J., Xu, M., Willmann, M. R., McCormick, K., Hu, T., Yang, L., Starker, C. G., Voytas, D. F., Meyers, B. C. and Poethig, R. S.** (2018a). Threshold-dependent repression of SPL gene expression by miR156/miR157 controls vegetative phase change in *Arabidopsis thaliana*. *PLoS Genet.* **14**, e1007337. doi:10.1371/journal.pgen.1007337
- He, L., Wu, W., Zinta, G., Yang, L., Wang, D., Liu, R., Zhang, H., Zheng, Z., Huang, H., Zhang, Q. et al.** (2018b). A naturally occurring epiallele associates with leaf senescence and local climate adaptation in *Arabidopsis* accessions. *Nat. Commun.* **9**, 460. doi:10.1038/s41467-018-02839-3
- Hudson, C. J., Freeman, J. S., Jones, R. C., Potts, B. M., Wong, M. M. L., Weller, J. L., Hecht, V. F. G., Poethig, R. S. and Vaillancourt, R. E.** (2014). Genetic control of heterochrony in *Eucalyptus globulus*. *G3* **4**, 1235-1245. doi:10.1534/g3.114.011916
- Huijser, P. and Schmid, M.** (2011). The control of developmental phase transitions in plants. *Development* **138**, 4117-4129. doi:10.1242/dev.063511
- James, S. A. and Bell, D. T.** (2001). Leaf morphological and anatomical characteristics of heteroblastic *Eucalyptus globulus* ssp. *globulus* (Myrtaceae). *Aust. J. Bot.* **49**, 259. doi:10.1071/BT99044
- Jiao, W.-B. and Schneeberger, K.** (2020). Chromosome-level assemblies of multiple *Arabidopsis* genomes reveal hotspots of rearrangements with altered evolutionary dynamics. *Nat. Commun.* **11**, 989. doi:10.1038/s41467-020-14779-y
- Jiménez-Gómez, J. M., Wallace, A. D. and Maloof, J. N.** (2010). Network analysis identifies *ELF3* as a QTL for the shade avoidance response in *Arabidopsis*. *PLoS Genet.* **6**, e1001100. doi:10.1371/journal.pgen.1001100
- Jordan, G. J., Potts, B. M., Chalmers, P. and Wiltshire, R. J. E.** (2000). Quantitative genetic evidence that the timing of vegetative phase change in *Eucalyptus globulus* ssp. *globulus* is an adaptive trait. *Aust. J. Bot.* **48**, 561-567.
- Jung, J.-H., Ju, Y., Seo, P. J., Lee, J.-H. and Park, C.-M.** (2012). The *SOC1-SPL* module integrates photoperiod and gibberellic acid signals to control flowering time in *Arabidopsis*. *Plant J.* **69**, 577-588. doi:10.1111/j.1365-313X.2011.04813.x
- Jung, J.-H., Lee, S., Yun, J., Lee, M. and Park, C.-M.** (2014). The miR172 target *TOE3* represses *AGAMOUS* expression during *Arabidopsis* floral patterning. *Plant Sci.* **215-216**, 29-38. doi:10.1016/j.plantsci.2013.10.010
- Katoh, K.** (2002). MAFFT: a novel method for rapid multiple sequence alignment based on fast Fourier transform. *Nucleic Acids Res.* **30**, 3059-3066. doi:10.1093/nar/gkf436
- Kawakatsu, T., Huang, S.-C., Jupe, F., Sasaki, E., Schmitz, R. J., Ulrich, M. A., Castanon, R., Nery, J. R., Barragan, C., He, Y. et al.** (2016). Epigenomic diversity in a global collection of *Arabidopsis thaliana* accessions. *Cell* **166**, 492-505. doi:10.1016/j.cell.2016.06.044
- Lawrence, E. H., Springer, C. J., Helliker, B. R. and Poethig, R. S.** (2021). MicroRNA156-mediated changes in leaf composition lead to altered photosynthetic traits during vegetative phase change. *New Phytol.* **231**, 1008-1022. doi:10.1111/nph.17007
- Leichty, A. R. and Poethig, R. S.** (2019). Development and evolution of age-dependent defenses in ant-acacias. *Proc. Natl. Acad. Sci. USA* **116**, 15596-15601. doi:10.1073/pnas.1900644116
- Lempe, J., Balasubramanian, S., Sureshkumar, S., Singh, A., Schmid, M. and Weigel, D.** (2005). Diversity of flowering responses in wild *Arabidopsis thaliana* strains. *PLoS Genet.* **1**, e6. doi:10.1371/journal.pgen.0010006
- Leopold, A. C.** (1961). Senescence in plant development. *Science* **134**, 1727-1732. doi:10.1126/science.134.3492.1727
- Levy, Y. Y. and Dean, C.** (1998). The transition to flowering. *Plant Cell* **10**, 1973-1989. doi:10.1105/tpc.10.12.1973
- Li, J., Wang, Z., Hu, Y., Cao, Y. and Ma, L.** (2017). Polycomb group proteins RING1A and RING1B regulate the vegetative phase transition in *Arabidopsis*. *Front. Plant Sci.* **8**, 867. doi:10.3389/fpls.2017.00867
- Lindenbaum, P.** (2015). Jvarkit: java-based utilities for Bioinformatics. figshare. Journal contribution. doi:10.6084/m9.figshare.1425030.v1
- Livak, K. J. and Schmittgen, T. D.** (2001). Analysis of relative gene expression data using real-time quantitative PCR and the 2^{-ΔΔCT} method. *Methods* **25**, 402-408. doi:10.1006/meth.2001.1262
- Love, M. I., Huber, W. and Anders, S.** (2014). Moderated estimation of fold change and dispersion for RNA-seq data with DESeq2. *Genome Biol.* **15**, 550. doi:10.1186/s13059-014-0550-8
- Martínez-Berdeja, A., Stitzer, M. C., Taylor, M. A., Okada, M., Ezcurra, E., Runcie, D. E. and Schmitt, J.** (2020). Functional variants of *DOG1* control seed chilling responses and variation in seasonal life-history strategies in *Arabidopsis thaliana*. *Proc. Natl. Acad. Sci. USA* **117**, 2526-2534. doi:10.1073/pnas.1912451117
- Mishler, B. D.** (1986). Ontogeny and phylogeny in *Tortula* (Musci: Pottiaceae). *Syst. Bot.* **11**, 189. doi:10.2307/2418957
- Nakano, Y., Kusunoki, K., Maruyama, H., Enomoto, T., Tokizawa, M., Iuchi, S., Kobayashi, M., Kochian, L. V., Koyama, H. and Kobayashi, Y.** (2020). A single-population GWAS identified AtMATE expression level polymorphism caused by promoter variants is associated with variation in aluminum tolerance in a local *Arabidopsis* population. *Plant Direct* **4**, e00250. doi:10.1002/pld3.250
- Nguyen, S. T. T., Greaves, T. and McCurdy, D. W.** (2017). Heteroblastic Development of transfer cells is controlled by the microRNA miR156/SPL module. *Plant Physiol.* **173**, 1676-1691. doi:10.1104/pp.16.01741
- Picó, S., Ortiz-Marchena, M. I., Merini, W. and Calonje, M.** (2015). Deciphering the role of POLYCOMB REPRESSIVE COMPLEX1 variants in regulating the acquisition of flowering competence in *Arabidopsis*. *Plant Physiol.* **168**, 1286-1297. doi:10.1104/pp.15.00073
- Poethig, R. S.** (1990). Phase change and the regulation of shoot morphogenesis in plants. *Science* **250**, 923-930. doi:10.1126/science.250.4983.923
- Ponnu, J., Schlereth, A., Zacharak, V., Dziato, M. A., Abel, C., Feil, R., Schmid, M. and Wahl, V.** (2020). The trehalose 6-phosphate pathway impacts vegetative phase change in *Arabidopsis thaliana*. *Plant J.* **104**, 768-780. doi:10.1111/tpj.14965
- Rosas, U., Mei, Y., Xie, Q., Banta, J. A., Zhou, R. W., Seufferheld, G., Gerard, S., Chou, L., Bhambhra, N., Parks, J. D. et al.** (2014). Variation in *Arabidopsis* flowering time associated with cis-regulatory variation in *CONSTANS*. *Nat. Commun.* **5**, 3651. doi:10.1038/ncomms4651
- Rose, K. M. E., Mickelbart, M. V. and Jacobs, D. F.** (2019). Plasticity of phenotype and heteroblasty in contrasting populations of *Acacia koa*. *Ann. Bot.* **124**, 399-409. doi:10.1093/aob/mcz083
- Rubin, M. J., Brock, M. T., Davis, S. J. and Weinig, C.** (2019). QTL underlying circadian clock parameters under seasonally variable field settings in *Arabidopsis thaliana*. *G3* **9**, 1131-1139. doi:10.1534/g3.118.200770
- Sasaki, E., Kawakatsu, T., Ecker, J. R. and Nordborg, M.** (2019). Common alleles of *CMT2* and *NRPE1* are major determinants of CHH methylation variation in *Arabidopsis thaliana*. *PLoS Genet.* **15**, e1008492. doi:10.1371/journal.pgen.1008492
- Scheres, B. and van der Putten, W. H.** (2017). The plant perceptron connects environment to development. *Nature* **543**, 337-345. doi:10.1038/nature22010
- Schindelin, J., Arganda-Carreras, I., Frise, E., Kaynig, V., Longair, M., Pietzsch, T., Preibisch, S., Rueden, C., Saalfeld, S., Schmid, B. et al.** (2012). Fiji: An open-source platform for biological-image analysis. *Nat. Methods* **9**, 676-682. doi:10.1038/nmeth.2019
- Schwartz, C., Balasubramanian, S., Warthmann, N., Michael, T. P., Lempe, J., Sureshkumar, S., Kobayashi, Y., Maloof, J. N., Borevitz, J. O., Chory, J. et al.** (2009). Cis-regulatory changes at *FLOWERING LOCUS T* mediate natural variation in flowering responses of *Arabidopsis thaliana*. *Genetics* **183**, 723-732. doi:10.1534/genetics.109.104984
- Sen, S. and Churchill, G. A.** (2001). A statistical framework for quantitative trait mapping. *Genetics* **159**, 371-387. doi:10.1093/genetics/159.1.371
- Sheldon, C. C., Rouse, D. T., Finnegan, E. J., Peacock, W. J. and Dennis, E. S.** (2000). The molecular basis of vernalization: the central role of *FLOWERING LOCUS C (FLC)*. *Proc. Natl. Acad. Sci. USA* **97**, 3753-3758. doi:10.1073/pnas.97.7.3753
- Shindo, C., Aranzana, M. J., Lister, C., Baxter, C., Nicholls, C., Nordborg, M. and Dean, C.** (2005). Role of *FRIGIDA* and *FLOWERING LOCUS C* in determining variation in flowering time of *Arabidopsis*. *Plant Physiol.* **138**, 1163-1173. doi:10.1104/pp.105.061309
- Simon, M., Loudet, O., Durand, S., Bérard, A., Brunel, D., Sennesal, F.-X., Durand-Tardif, M., Pelletier, G. and Camilleri, C.** (2008). Quantitative trait loci mapping in five new large recombinant inbred line populations of *Arabidopsis thaliana* genotyped with consensus single-nucleotide polymorphism markers. *Genetics* **178**, 2253-2264. doi:10.1534/genetics.107.083899
- Stief, A., Altmann, S., Hoffmann, K., Pant, B. D., Scheible, W.-R. and Bäurle, I.** (2014). *Arabidopsis* miR156 regulates tolerance to recurring environmental stress through *SPL* transcription factors. *Plant Cell* **26**, 1792-1807. doi:10.1105/tpc.114.123851
- Symonds, V. V., Godoy, A. V., Alconada, T., Botto, J. F., Juenger, T. E., Casal, J. J. and Lloyd, A. M.** (2005). Mapping quantitative trait loci in multiple populations of *Arabidopsis thaliana* identifies natural allelic variation for trichome density. *Genetics* **169**, 1649-1658. doi:10.1534/genetics.104.031948
- Telfer, A., Bollman, K. M. and Poethig, R. S.** (1997). Phase change and the regulation of trichome distribution in *Arabidopsis thaliana*. *Development* **124**, 645-654. doi:10.1242/dev.124.3.645

- Thomas, H., Ougham, H. J., Wagstaff, C. and Stead, A. D. (2003). Defining senescence and death. *J. Exp. Bot.* **54**, 1127-1132. doi:10.1093/jxb/erg133
- Tsuzuki, M., Futagami, K., Shimamura, M., Inoue, C., Kunimoto, K., Oogami, T., Tomita, Y., Inoue, K., Kohchi, T., Yamaoka, S. et al. (2019). An early arising role of the microRNA156/529-SPL module in reproductive development revealed by the liverwort *Marchantia polymorpha*. *Curr. Biol.* **29**, 3307-3314.e5. doi:10.1016/j.cub.2019.07.084
- Varkonyi-Gasic, E., Wu, R., Wood, M., Walton, E. F. and Hellens, R. P. (2007). Protocol: a highly sensitive RT-PCR method for detection and quantification of microRNAs. *Plant Methods* **3**, 12. doi:10.1186/1746-4811-3-12
- Wahl, V., Ponnur, J., Schlereth, A., Arrivault, S., Langenecker, T., Franke, A., Feil, R., Lunn, J. E., Stitt, M. and Schmid, M. (2013). Regulation of flowering by trehalose-6-phosphate signaling in *Arabidopsis thaliana*. *Science* **339**, 704-707. doi:10.1126/science.1230406
- Wang, J.-W. (2014). Regulation of flowering time by the miR156-mediated age pathway. *J. Exp. Bot.* **65**, 4723-4730. doi:10.1093/jxb/eru246
- Wang, H. and Wang, H. (2015). The miR156/SPL module, a regulatory hub and versatile toolbox, gears up crops for enhanced agronomic traits. *Mol. Plant* **8**, 677-688. doi:10.1016/j.molp.2015.01.008
- Wang, J.-W., Czech, B. and Weigel, D. (2009). miR156-regulated SPL transcription factors define an endogenous flowering pathway in *Arabidopsis thaliana*. *Cell* **138**, 738-749. doi:10.1016/j.cell.2009.06.014
- Wang, J.-W., Park, M. Y., Wang, L.-J., Koo, Y., Chen, X.-Y., Weigel, D. and Poethig, R. S. (2011). miRNA control of vegetative phase change in trees. *PLoS Genet.* **7**, e1002012. doi:10.1371/journal.pgen.1002012
- Wang, L., Zhou, C.-M., Mai, Y., Li, L.-Z., Gao, J., Shang, G.-D., Lian, H., Han, L., Zhang, T.-Q., Tang, H. et al. (2019). A spatiotemporally regulated transcriptional complex underlies heteroblastic development of leaf hairs in *Arabidopsis thaliana*. *EMBO J.* **38**, e100063. doi:10.15252/embj.2018100063
- Wareing, P. F. (1959). Problems of juvenility and flowering in trees. *J. Linn. Soc. Lond. Bot.* **56**, 282-289. doi:10.1111/j.1095-8339.1959.tb02504.x
- Willmann, M. R. and Poethig, R. S. (2011). The effect of the floral repressor FLC on the timing and progression of vegetative phase change in *Arabidopsis*. *Development* **138**, 677-685. doi:10.1242/dev.057448
- Wiltshire, R. J. E., Potts, B. M. and Reid, J. B. (1991). A paedomorphocline in *Eucalyptus*: natural variation in the *E. risdonii*/*E. tenuiramis* complex. *Aust. J. Bot.* **39**, 545-566. doi:10.1071/BT9910545
- Wiltshire, R. J. E., Reid, J. B. and Potts, B. M. (1998). Genetic control of reproductive and vegetative phase change in the *Eucalyptus risdonii*-*E. tenuiramis* complex. *Aust. J. Bot.* **46**, 45-63. doi:10.1071/BT97020
- Wu, G., Park, M. Y., Conway, S. R., Wang, J.-W., Weigel, D. and Poethig, R. S. (2009). The sequential action of miR156 and miR172 regulates developmental timing in *Arabidopsis*. *Cell* **138**, 750-759. doi:10.1016/j.cell.2009.06.031
- Xie, Y., Zhou, Q., Zhao, Y., Li, Q., Liu, Y., Ma, M., Wang, B., Shen, R., Zheng, Z. and Wang, H. (2020). FHY3 and FAR1 integrate light signals with the miR156-SPL module-mediated aging pathway to regulate *Arabidopsis* flowering. *Mol. Plant* **13**, 483-498. doi:10.1016/j.molp.2020.01.013
- Xu, M., Hu, T., Smith, M. R. and Poethig, R. S. (2015). Epigenetic regulation of vegetative phase change in *Arabidopsis*. *Plant Cell* **28**, 28-41. doi:10.1105/tpc.15.00854
- Xu, M., Hu, T., Zhao, J., Park, M.-Y., Earley, K. W., Wu, G., Yang, L. and Poethig, R. S. (2016). Developmental functions of miR156-Regulated SQUAMOSA PROMOTER BINDING PROTEIN-LIKE (SPL) genes in *Arabidopsis thaliana*. *PLoS Genet.* **12**, e1006263. doi:10.1371/journal.pgen.1006263
- Xu, Y., Qian, Z., Zhou, B. and Wu, G. (2019). Age-dependent heteroblastic development of leaf hairs in *Arabidopsis*. *New Phytol.* **224**, 741-748. doi:10.1111/nph.16054
- Xu, M., Hu, T. and Poethig, R. S. (2021). Low light intensity delays vegetative phase change. *Plant Physiol.* **187**, 1177-1188. doi:10.1093/plphys/kiab243
- Yuan, J. and Kessler, S. A. (2019). A genome-wide association study reveals a novel regulator of ovule number and fertility in *Arabidopsis thaliana*. *PLoS Genet.* **15**, e1007934. doi:10.1371/journal.pgen.1007934
- Zhang, J., Fu, X.-X., Li, R.-Q., Zhao, X., Liu, Y., Li, M.-H., Zwaenepoel, A., Ma, H., Goffinet, B., Guan, Y.-L. et al. (2020). The hornwort genome and early land plant evolution. *Nat. Plants* **6**, 107-118. doi:10.1038/s41477-019-0588-4
- Zhu, Q.-H. and Helliwell, C. A. (2011). Regulation of flowering time and floral patterning by miR172. *J. Exp. Bot.* **62**, 487-495. doi:10.1093/jxb/erq295

Figure S1

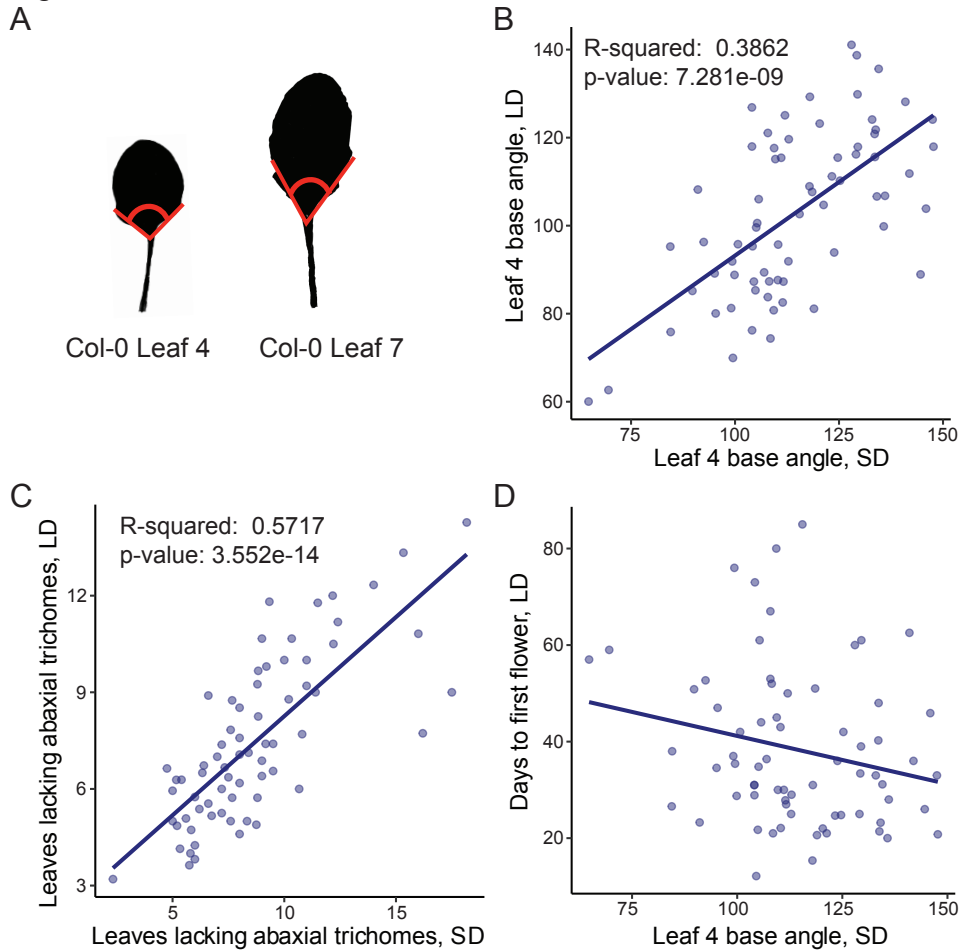


Fig. S1. Relationship between vegetative traits and flowering time in SD and LD.

(A) Leaves four and seven of the Col-0 accession, with measures of leaf base angle indicated in red.

(B) Correlation between leaf four base angle in LD and SD conditions.

(C) Correlation between leaves lacking abaxial trichomes in SD and leaves lacking abaxial trichomes in LD conditions.

(D) Correlation between leaf four base angle in SD and days to opening of first flower in LD conditions. Blue lines shown are linear regression model; R^2 and p -values from linear regression analysis displayed in upper right corner of each panel.

Figure S2

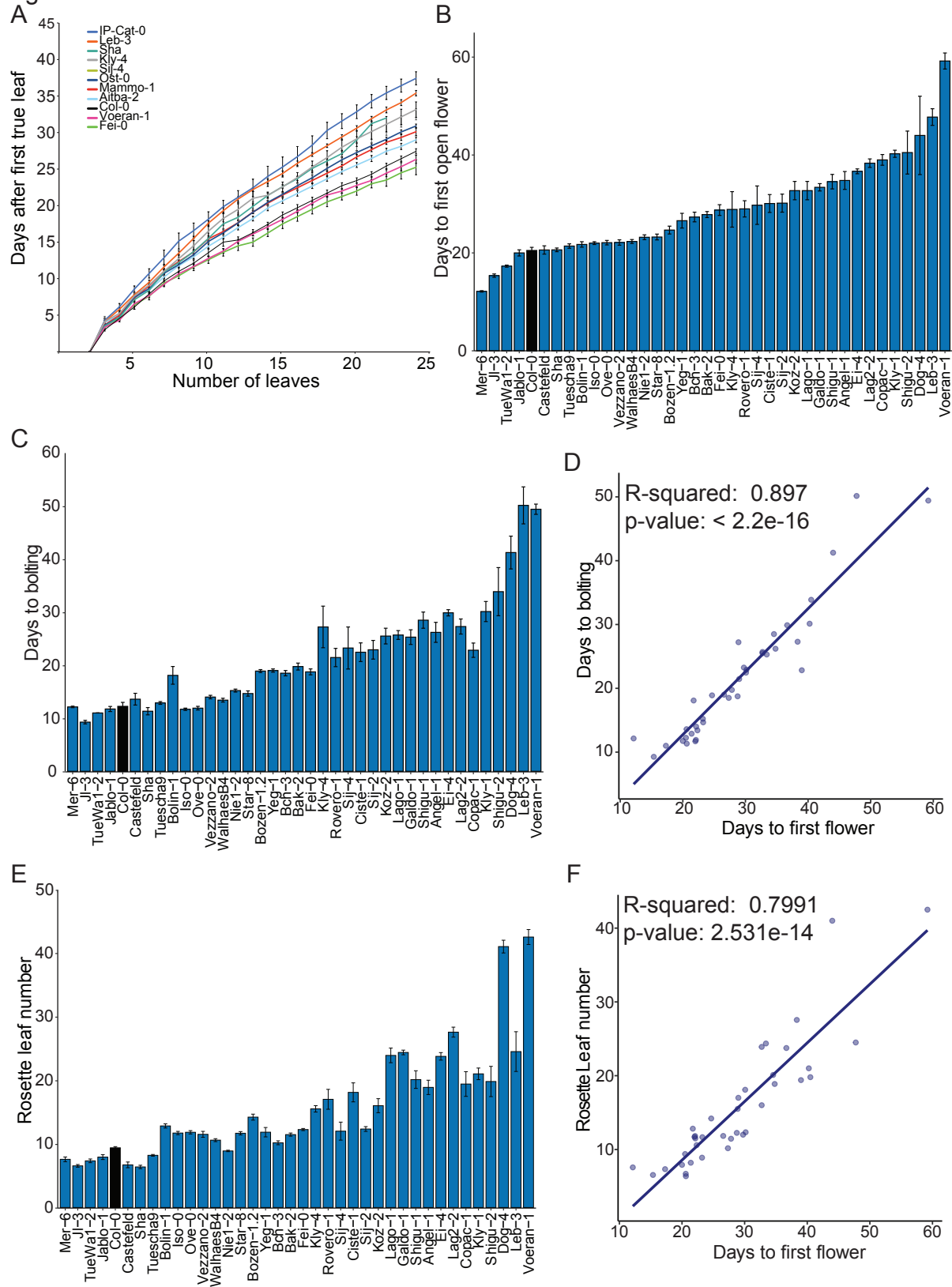


Fig. S2. Assessment of reproductive phase transition for scoring timing of timing of reproductive phase transition in natural accessions.

(A) Rate of leaf initiation in a group of selected accessions. Data show number of visible leaves and days after the appearance of first true leaves.

(B) Days to first open flower in a group of selected accessions.

(C) Days to bolting in a group of selected accessions, in same order as S2B.

(D) Correlation between days to opening of first flower and days to bolting in LD conditions. Blue lines shown are linear regression model; R^2 and p -values from linear regression analysis displayed in upper right corner of each panel.

(E) Rosette leaf number in a group of selected accessions, in same order as S2B.

(F) Correlation between rosette leaf number and days to opening of first flower. Blue lines shown are linear regression model; R^2 and p -values from linear regression analysis displayed in upper right corner of each panel.

Figure S3

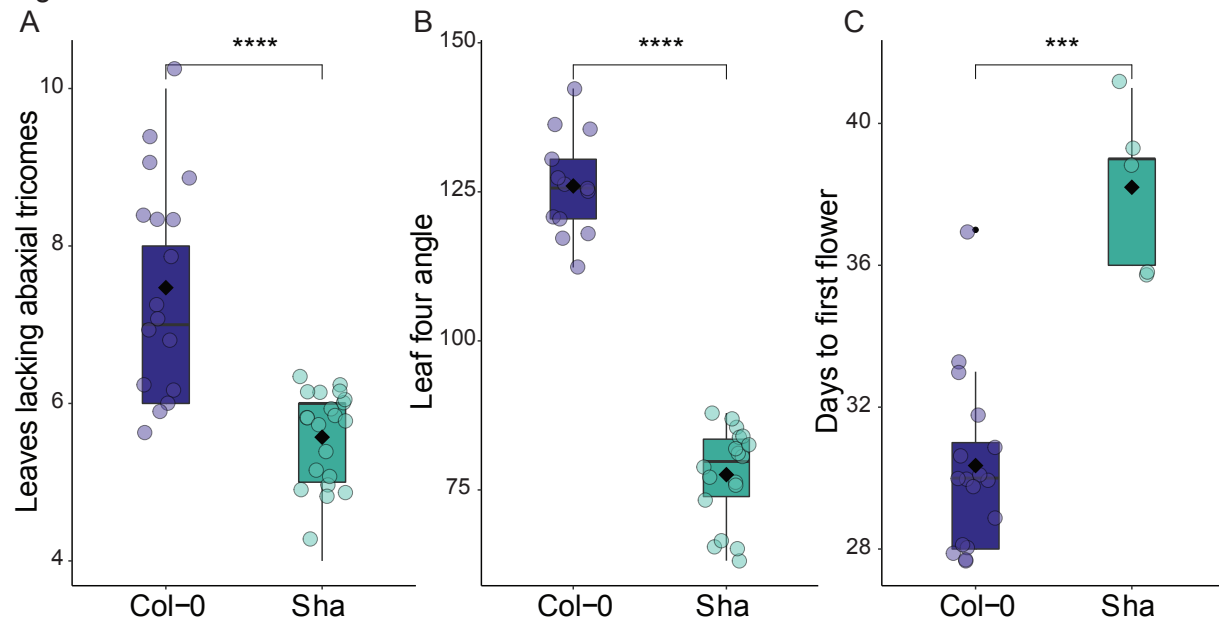


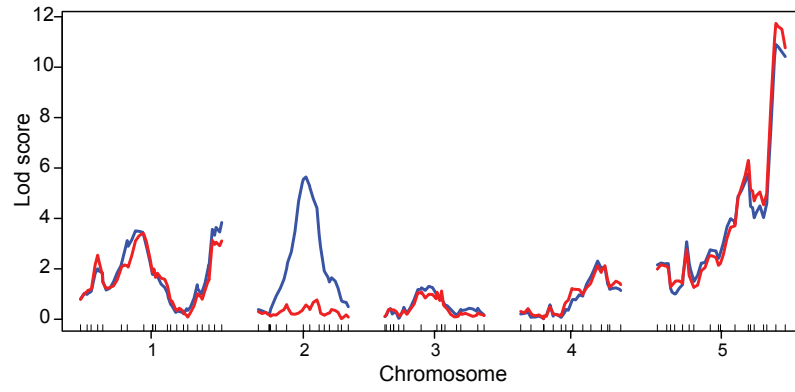
Fig. S3. Timing of vegetative phase change of Sha and Col-0 in non-vernalized conditions.

(A-D) The number of leaves lacking abaxial trichomes (A), leaf four base angle (B), and days to first open flower (C) in non-vernalized LD conditions. Significance was determined by two-tailed Student's *t*-test (** $p < 0.001$, **** $p < 0.0001$).

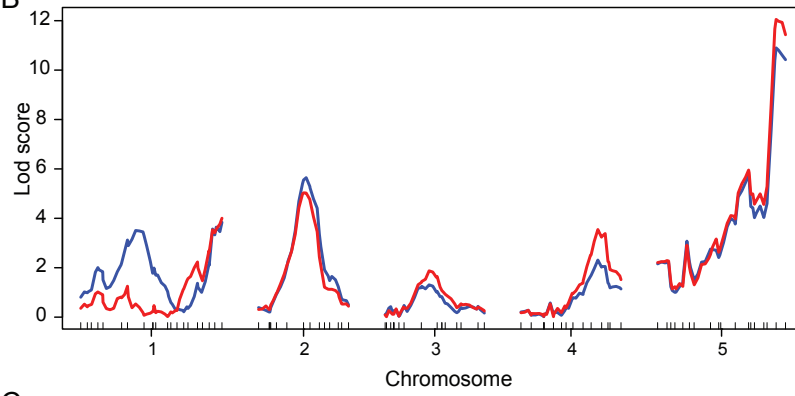
Blue/green dots indicate biological replicates; black dot indicate outliers; center line marks the median value; boxes outline the first and third quartiles, whiskers mark minimum and maximum values.

Figure S4

A



B



C

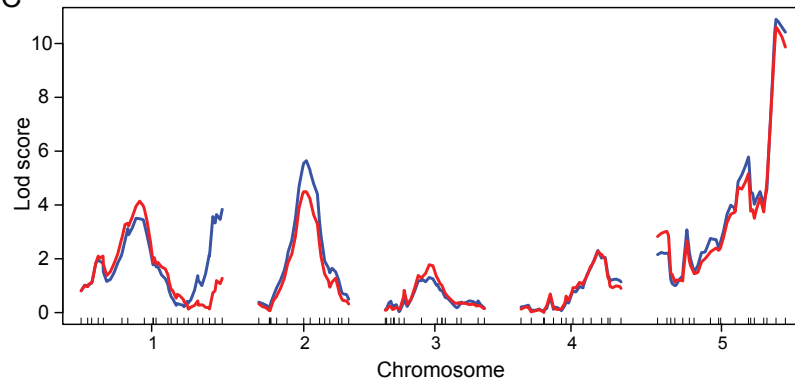


Fig. S4. Covariate analysis of leaves lacking abaxial trichomes and QTLs in Sha X Col-0 RILs.

(A) Covariate analysis using the peak coordinate of the QTL on chromosome two. Red lines are LOD scores based on leaves lacking abaxial trichomes using maximum likelihood via the EM algorithm. Blue lines are the LOD score based on a genome scan for number of leaves lacking abaxial trichomes with the effects of each QTL peak on chromosome five incorporated as an interacting covariate.

(B-C) Covariate analysis using the peak coordinates of the QTLs on chromosome one. Red lines are LOD scores based on leaves lacking abaxial trichomes using maximum likelihood via the EM algorithm. Blue lines are the LOD score based on a genome scan for number of leaves lacking abaxial trichomes with the effects of each QTL peak on chromosome five incorporated as an interacting covariate.

Table S1. Catalog numbers and phenotypic data of natural accessions used in this study

[Click here to download Table S1](#)

Table S2. Phenotypic and genotypic data of RIL lines used in this study

[Click here to download Table S2](#)

Table S3. Primers used in this study

smRNA RT-qPCR		
Name	Use	Sequence (5'-3')
miR156 RT	miR156 reverse transcription	GTCGTATCCAGTGCAGGGTCCGAGGTATTTCGCACTGGA TACGACGTGCTC
miR172 RT	miR172 reverse transcription	GTCGTATCCAGTGCAGGGTCCGAGGTATTTCGCACTGGA TACGACATGCAG
miR156 F	miR156 qPCR	GCGGCGGTGACAGAAGAGAGT
miR172 F	miR172 qPCR	CGGCGGAGAATCTTGATGATGC
Universal R	miRNA qPCR	GTGCAGGGTCCGAGGT
SnoR101 F	SnoR101 qPCR	CTTCACAGGTAAGTTCGCTTG
SnoR101 R	SnoR101 RT and qPCR	AGCATCAGCAGACCAGTAGTT
mRNA RT-qPCR		
Name	Use	Sequence (5'-3')
oligo dT	Reverse transcription	TTTTTTTTTTTTTTTTTTTTTTTT
ACT2-F	qPCR	GCACCTGTCTTCTTACCG
ACT2-R	qPCR	AACCCTCGTAGATTGGCACA
SPL2-F	qPCR	TTTCCGATACCGAGCACAATAG
SPL2-F	qPCR	TACGGGTTGGAGGTTGCTTGAGG
SPL3-F	qPCR	ATGAGTATGAGAAGAAGCAAAGCG
SPL3-R	qPCR	TCCACTACTACTTGTAGCTTTACCT
SPL9-F	qPCR	GGAATTTGACCTAGAGAAAAGGAGTT
SPL9-R	qPCR	GCATCACCATTTTCGTAAAGCGAAG
SPL10-F	qPCR	CAGACAAAGGTGTGGGAGAATGCTC
SPL10-R	qPCR	TAGGGAAAGTGCCAAATATTGGCG
SPL13-F	qPCR	GGGTTTTCAAGGTAGCAAATTGCT
SPL13-R	qPCR	ACCAACAACATAGCTCTGGCTCTG
SPL11-F	qPCR	AGTCCAAGTTTCAACTTCATGGCG
SPL11-F	qPCR	GAACAGAGTAGAGAAAATGGCTGC
SPL15-F	qPCR	TGAATGTTTTATCACATGGAAGCTC
SPL15-R	qPCR	TCATCGAGTCGAAACCAGAAGATG
miR156C-F	qPCR	AAAAGCCTCAGATCTAACTCCAACAC
miR156C-R	qPCR	GCGTTTCTCTTAAAATTTGTCCCAAAACT
miR156A-F	qPCR	CTTCGTTCTCTATGTCTCAATCTCTC
miR156A-R	qPCR	TGATTAAAGGCTAAAGGTCTCCTC
TOE1-F	qPCR	CGAGTTATAATAATCCCGCCGAG
TOE1-R	qPCR	TTAAGGGTGTGGATAAAAGT
TOE2-F	qPCR	ATGGAGAACCACATGGCTGC
TOE2-R	qPCR	GGTGCTGTAGCTGCTACGGC
TOE3-F	qPCR	CTCACCCGATCATCACGAAG
TOE3-R	qPCR	TATTGAAACCGGACCAACGA

Table S4. DESeq and SNPEff results for Sha QTLs

[Click here to download Table S4](#)